AD-A060 640   VIRGINIA COMMONWEALTH UNIV RICHMOND DEPT OF PHYSICS   F/G 10/2
OPTICAL PROPERTIES OF SEMICONDUCTORS: SOLAR CELL MATERIALS.(U)
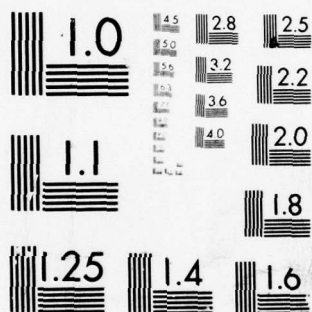AUG 78 E SHILES   AFOSR-78-3591
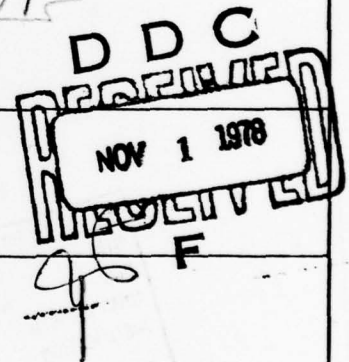UNCLASSIFIED   AFOSR-TR-78-1412   NL

1 OF 1

AD
A060640

END
DATE
FILMED
1 —79
DDC

MICROCOPY RESOLUTION TEST CHART

NATIONAL BUREAU OF STANDARDS-1963-A

SECURITY CLASSIFICATION OF THIS PAGE (When Data Entered)

REPORT DOCUMENTATION PAGE	READ INSTRUCTIONS BEFORE COMPLETING FORM

1. REPORT NUMBER	2. GOVT ACCESSION NO.	3. RECIPIENT'S CATALOG NUMBER
AFOSR-TR-78-1412		

4. TITLE (and Subtitle)

OPTICAL PROPERTIES OF SEMICONDUCTORS: SOLAR CELL MATERIALS.

5. TYPE OF REPORT & PERIOD COVERED

FINAL rept.
15 May 1978 - 15 Aug 78,

6. PERFORMING ORG. REPORT NUMBER

7. AUTHOR(s)

EUGENE SHILES

8. CONTRACT OR GRANT NUMBER(s)

AFOSR-78-3591

9. PERFORMING ORGANIZATION NAME AND ADDRESS

VIRGINIA COMMONWEALTH UNIVERSITY
DEPARTMENT OF PHYSICS
901 WEST FRANKLIN ST/RICHMOND, VA 23284

10. PROGRAM ELEMENT, PROJECT, TASK AREA & WORK UNIT NUMBERS

2308D9   D9
61102F

11. CONTROLLING OFFICE NAME AND ADDRESS

AIR FORCE OFFICE OF SCIENTIFIC RESEARCH/NA
BLDG 410
BOLLING AIR FORCE BASE, D C 20332

12. REPORT DATE

1978 15 Aug 78

13. NUMBER OF PAGES

73

14. MONITORING AGENCY NAME & ADDRESS(if different from Controlling Office)

15. SECURITY CLASS. (of this report)

UNCLASSIFIED

15a. DECLASSIFICATION/DOWNGRADING SCHEDULE

LEVEL

16. DISTRIBUTION STATEMENT (of this Report)

Approved for public release; distribution unlimited.

17. DISTRIBUTION STATEMENT (of the abstract entered in Block 20, if different from Report)

DDC
NOV 1 1978
F

18. SUPPLEMENTARY NOTES

19. KEY WORDS (Continue on reverse side if necessary and identify by block number)

OPTICAL PROPERTIES
OPTICAL CONSTANTS
SILICON
GALLIUM ARSENIDE

20. ABSTRACT (Continue on reverse side if necessary and identify by block number)

The optical properties of the semiconductors silicon and gallium arsenide have been examined by a Kramers-Kronig analysis of the available experimental measurements of the optical constants (reflectivity, extinction coefficient, index of refraction, and dielectric function) for these materials. The results include the full range of optical electronic excitations, from infrared through X-rays, and have been examined by the evaluation of various sum rules. The sum rules are well satisfied by the resulting silicon data, and the results are consistent with the various experimental measurements. There is some question concerning the data in

DD FORM 1473
1 JAN 73

UNCLASSIFIED 410 911

SECURITY CLASSIFICATION OF THIS PAGE (When Data Entered)

AD A060640

DDC FILE COPY

the region of band-to-band transitions (visible and ultra-violet); the resolution must await further experimental measurements of reflectivity and/or dielectric function in this spectral range. The silicon work constitutes the first part of this report. For gallium arsenide, the sum rules analysis indicates that the available experimental measurements of the absorption of gallium and arsenic may be too small in the X-ray region at energies less than the onset of L-shell core electron excitations. Also the data is incomplete in the region just above the L-shell threshold. Comparison of the final results with various experimental measurements also indicate that the available normal-incidence reflectivity data in the region of band-to-band transitions may be inaccurate (values too small). The gallium arsenide calculation and the above mentioned problems are described in the second part of this report. The work is continuing, in an attempt to locate more experimental data and to define more closely the spectral regions were the presently available data is inaccurate.

where

OPTICAL PROPERTIES OF SEMICONDUCTORS:
SOLAR CELL MATERIALS

Final Report
covering period 15 May 78 - 15 Aug 78

by
EUGENE SHILES, PhD
(Principal Investigator)
Dept. of Physics, Virginia Commonwealth University
Richmond, VA 23284

78 10 16 129

OBJECTIVES

The study was intended to calculate, by a Kramers-Kronig analysis of available experimental data, the optical constants of the semiconductors silicon and gallium arsenide for the full range of optical electronic excitations (infrared to X-ray), and to evaluate the results using various sum rules.

STATUS OF THE EFFORT

The calculation is complete, consistent with the experimental data that the researchers were able to obtain. As described in the report, further improvement awaits the availability of more accurate experimental measurements in various frequency ranges, particularly in the case of gallium arsenide.

PUBLICATION

The work will be submitted for publication in Physical Review B, probably in two parts (two articles).

PROFESSIONAL PERSONNEL

Dr. Eugene Shiles, Principal Investigator
Dept. of Physics
Virginia Commonwealth University
Richmond, VA

Dr. David Y. Smith
Solid State Sciences Division
Argonne National Laboratory
Argonne, Ill.

INTERACTIONS

The principal investigator spent several weeks at Argonne National Laboratory, at the beginning and near the end of the grant period.

INVENTIONS, PATENTS

No inventions or patents are associated with this work.

Note: In the text, there are separately numbered lists of figures and references for the two parts of the report; they are included at the end of each part, respectively. The pages of each part are also numbered separately.

78 10 16 129

ABSTRACT

The optical properties of the semiconductors silicon and gallium arsenide have been examined by a Kramers-Kronig analysis of the available experimental measurements of the optical constants (reflectivity, extinction coefficient, index of refraction, and dielectric function) for these materials. The results include the full range of optical electronic excitations, from infrared through X-rays, and have been examined by the evaluation of various sum rules.

The sum rules are well satisfied by the resulting silicon data, and the results are consistent with the various experimental measurements. There is some question concerning the data in the region of band-to-band transitions (visible and ultra-violet); the resolution must await further experimental measurements of reflectivity and/or dielectric function in this spectral range. The silicon work constitutes the first part of this report.

For gallium arsenide, the sum rules analysis indicates that the available experimental measurements of the absorption of gallium and arsenic may be too small in the X-ray region at energies less than the onset of L-shell core electron excitations. Also the data is incomplete in the region just above the L-shell threshold. Comparison of the final results with various experimental measurements also indicate that the available normal-incidence reflectivity data in the region of band-to-band transitions may be inaccurate (values too small). The gallium arsenide calculation and the above mentioned problems are described in the second part of this report. The work is continuing, in an attempt to locate more experimental data and to define more closely the spectral regions where the presently available data is inaccurate.

(Optical Constants of Silicon)

1. INTRODUCTION

The optical constants of a material, which consist of the reflectivity, index of refraction, extinction coefficient (or the related absorption coefficient), and dielectric constant are of general scientific and technical interest. They are a function of frequency (or photon energy) of the incident electromagnetic radiation; for various reasons, the quantities cannot be measured at all incident energies, and the technique of Kramers-Kronig integration may be used to extend the available data to the full spectrum. Such self-consistent calculations were pioneered by Philipp and Ehrenreich[1] in a study of the optical properties of aluminum.

Philipp's analysis[2] of the optical properties of pure silicon includes an incomplete evaluation of the Kramer-Kronig integral and an incorrect application of sum rules. Both of these problems are described in detail below. In the present work we propose, by a complete Kramers-Kronig analysis and a correct application of the sum rules (including some recent advances in the theory of sum rules[3,4]), to correct the data where it is erroneous, put on a firmer basis that data which is accurate, and extend the results to incident photon energies above the K-edge. In this calculation we treat only pure single crystal silicon at room temperature $(300^{\circ}K)$ and the results include the full range of optical electronic excitations (infra-red through X-rays).

For normal incidence reflection we have the complex quantity

$$\tilde{r}(\omega) = r(\omega)e^{i\theta(\omega)}, \quad R(\omega) = r^2(\omega), \qquad (1)$$

where $R(\omega)$ is the fractional change in intensity of the reflected beam as compared to the incident beam and $\theta(\omega)$ is the change of phase of the electromagnetic wave upon reflection; the dependence on incident photon energy ω has been indicated. The complex index of refraction is

$$\tilde{N}(\omega) = n(\omega) + i\kappa(\omega), \tag{2}$$

where $n(\omega)$, the index of refraction, measures the change in velocity of the wave when it enters the material ($v \simeq c/n$), and $\kappa(\omega)$, the extinction coefficient, measures the loss of amplitude of the wave as it passes through the material (change is proportional to $\exp(-2\pi\kappa x/\lambda)$, where λ is the wavelength and x is the distance traversed). We note here that the absorption coefficient α is related to κ by the expression $\alpha = 4\pi\kappa/\lambda$. In the limit of long wavelength (the region of interest for the study of optical properties) and in materials where the dielectric response is isotropic, the dielectric properties can be described by the complex dielectric constant involving only two numbers,

$$\tilde{\varepsilon}(\omega) = \varepsilon_1(\omega) + i\varepsilon_2(\omega), \tag{3}$$

where $\varepsilon_1(\omega)$, the real part, describes the polarization of the material, and $\varepsilon_2(\omega)$, the imaginary part, measures the energy lost by the electromagnetic wave, passing through the material, that is dissipated in the material. The pairs of functions (R,θ), (n,κ), and $(\varepsilon_1, \varepsilon_2)$ are related by the Kramer-Kronig integrals in such a way that one can calculate one quantity of a pair at any chosen energy if the other quantity of that pair is known at all energies.

If $R(\omega)$ is the known function, then the integral to be used to obtain $\theta(\omega)$ at a chosen energy ω_0 is

$$\theta(\omega_0) = \frac{\omega_0}{\pi} P \int_0^\infty \frac{\ln R(\omega)}{\omega^2 - \omega_0^2} d\omega \tag{4}$$

where P indicates that the principal value is to be taken in the integration around the pole. If $\kappa(\omega)$ is the known function, then one uses, to obtain $n(\omega)$ at chosen ω_0,

$$n(\omega_0) = 1 + \frac{2}{\pi} P \int_0^\infty \omega \frac{\kappa(\omega) d\omega}{\omega^2 - \omega_0^2} . \tag{5}$$

Similar expressions allow one to obtain $\kappa(\omega)$ from $n(\omega)$, $\varepsilon_1(\omega)$ from $\varepsilon_2(\omega)$, and $\varepsilon_2(\omega)$ from $\varepsilon_1(\omega)$.

If both quantities of any pair is known at any given energy, the others can be determined at that energy. The relations are

$$R(\omega) = \frac{(n(\omega) - 1)^2 + \kappa(\omega)^2}{(n(\omega) + 1)^2 + \kappa(\omega)^2} ,$$

$$\tan(\theta(\omega)) = \frac{-2\kappa(\omega)}{n(\omega)^2 + \kappa(\omega)^2 - 1} ,$$

$$\varepsilon_1(\omega) = n(\omega)^2 - \kappa(\omega)^2,$$

$$\varepsilon_2(\omega) = 2n(\omega) \kappa(\omega), \tag{6}$$

and various inversions of these expressions.

In a conductor such as aluminum, roughly speaking, the extinction coefficient $\kappa(\omega)$ cannot be measured accurately at frequencies below that of the plasma frequency of the conduction electrons (approx. 15.3 electron volts in aluminum in units of $h\omega$, where h is Planck's constant) and the reflectivity $R(\omega)$ cannot be measured accurately above the plasma frequency. Kramers-Kronig analysis can be used to combine the reflectivity data in the low region and the extinction data in the high region and obtain all the optical constants for the full spectrum. For a semiconductor, $R(\omega)$ is measurable below the plasma frequency (approx. 16.7 ev in silicon) and $\kappa(\omega)$ is measurable at the very low frequencies (below approx. 3 ev in silicon) and above the plasma frequency. The procedure, in both cases, is to start with one function, for example $R(\omega)$, using the available data in the measurable range and an approximation for the rest of the spectrum, and numerically evaluate the Kramers-Kronig integral (eq. (4) for $\theta(\omega)$, in this example). Then the other constants are determined from the expressions (6) and compared with experimental values in their measurable ranges. The result for $\kappa(\omega)$ (in our example where we started with $R(\omega)$) is then modified if necessary to match the experimental data, and another integration is done (eq. (5)), eventually reproducing $R(\omega)$ for the full spectrum. The procedure is then repeated using the improved data until a satisfactory match with all experiments is obtained. The initial data must be chosen carefully

to keep the number of iterations, hence the computational time, to a minimum. For the conductor aluminum it was found[5] that using $R(\omega)$ as a starting function allowed a reasonable determination of the optical constants in only one iteration. For the semiconductor silicon, $\kappa(\omega)$ may be a better starting function due to the availability of absorption data at both high and low incident energies.

Once the optical constants are known for the full spectrum, various sum rules can be used to test both the self-consistency of the results (correct Kramers-Kronig calculation) and the accuracy of the experimental data utilized. The "inertial" sum rule[4],

$$\int_0^\infty (n(\omega) - 1) d\omega = 0, \tag{7}$$

essentially tests for the self consistency of the index of refraction data, hence also the other constants evaluated in the same calculation. The f-sum rules are expressed

$$n_e = C \int_0^\infty \omega F(\omega) d\omega, \tag{8}$$

where $F(\omega)$ is one of the three quantities $\varepsilon_2(\omega)$, $2\kappa(\omega)$, or the energy loss function $-\text{Im}(1/\tilde{\varepsilon}(\omega)) = \varepsilon_2(\omega)/(\varepsilon_1^2(\omega) + \varepsilon_2^2(\omega))$, ω is the photon energy (in ev), and C is a constant depending on the density of electrons in the material (for silicon, $C \approx .009249$ ev^2). n_e is the number of electrons per atom participating in the optical properties ($n_e = 14$ for Si). Experimental data that is too large or too small will not give the predicted value for n_e.

Partial f-sum rules, that is, the evaluation of eq. (8) up to finite energy rather than infinity, can help to indicate whether the oscillator strength is properly distributed among the valence and the core electrons. In addition the three variations of the f-sum rules should not give the same value for the _partial_ sums[3], as we will discuss later.

We note here that the satisfaction of the sum rules is a necessary, but not sufficient, condition for the validity of the results; the data must be shown to fit the experiments in all important regions.

Philipp's[2] Kramers-Kronig calculation for silicon is incomplete in that it does not include the effects of the core electrons in the starting function. These effects show up, in silicon, as peaks in the absorption curve (also in the other optical constants) at about 100 ev (onset of L-shell electron excitation) and 1840 ev (onset of K-shell electron excitation). This in itself is not expected to affect the evaluation of the optical constants in the important region of the band to band transitions to a large extent, although a correction of this kind is of general scientific interest. Philipp's calculation was intended to account for the influence of an oxide layer on the silicon crystal sample during reflectivity measurements. Part of that calculation included forcing the f-sum rules on $\epsilon_2(\omega)$ and $-\text{Im}(1/\epsilon(\omega))$ to equal 4 (valence electrons) when integrated only up to an energy less than the onset of L-shell absorption. Recent studies[3] show that the two rules should not give the same value for this partial sum; we find that the $\epsilon_2(\omega)$ sum should

be about 4.15 and the $=\text{Im}(1/\varepsilon(\omega))$ sum should be about 4.05.
This could lead to an appreciable error in the earlier results.

The next section explains our choice of experimental data.
integration techniques, and iteration procedures for pure sili-
con, and presents our results.

2. KRAMERS-KRONIG ANALYSIS

The calculation was begun by constructing a complete set
of extinction coefficient $\kappa(\omega)$ data from $\omega = 0$ to $\omega \rightarrow \infty$, for
single-crystal silicon at 300°K. Experiments show a rapid drop
in absorption below about 3 ev, and we take $\kappa(\omega) = 0$ for $\omega < 1.05$
ev; this behavior is due to the scarcity of electrons in the
silicon conduction band at 300°K. For the range 1.05 ev to 3.4
ev, we used a curve that closely fits the data of Dash and Newman[6],
So and Vedam[7]. Azzam, Zaghloul, and Bashara[8], and the transmission
measurements of Philipp[2] (not the oxide-free calculation results).
Fig. 3 shows part of this curve. We note that the experiments of
So and Vedam and of Azzam, et al, are not a direct measurement of
absorption, but rather an ellipsometric method that leads to an
evaluation of the constants $n(\omega)$ and $\kappa(\omega)$ at a given frequency.
As an initial approximation in the region where $\kappa(\omega)$ cannot be
measured. the $\kappa(\omega)$ results of Philipp and Taft[9], obtained by a
partial Kramers-Kronig Analysis of reflectivity $R(\omega)$ measurements,
were used in the range 3 ev to 7 ev, and the curve was approximated
from 7 ev to 10.5 ev. The range 10.5 ev to 19 ev was obtained from
a smooth curve fitted to the data of Sasaki and Ishiguro[10], who
measured reflectance at the two angles of incidence 20° and 70° and
determined $n(\omega)$ and $\kappa(\omega)$ from this data. The range 19 ev to 30 ev

was approximated by assuming free electron behavior in the region just above the bulk plasmon frequency of 16.7 ev. We approximated the 30 ev to 99 ev region by connecting the curve at 30 ev to the experimental measurements of $\kappa(\omega)$ at 99 ev and above, and assuming a behavior similar to that of aluminum in this range. Here the valence (and conduction) electrons are essentially saturated, and the similarity of the cores in the two elements Si and Al lead us to expect similar behavior. The region of L-electron core excitations was obtained from the measurements of $\kappa(\omega)$ by Brown, et al[11], which include the range 95 ev to 210 ev. The X-ray range above 210 ev was obtained from tables of experimental values and theoretical calculations, all of which could be fit by a curve with very nearly the dependence $\kappa(\omega) \propto \omega^{-3.9}$ except near the onset of K-shell core excitations (at 1840 ev). The tables are those of reference 12,13,14,15,16,17, and 18; most of these tables give the mass absorption coefficient, which easily converts to $\kappa(\omega)$. The function $\kappa(\omega) = A\omega^{-4}$ was used as a high energy extrapolation for the integration from $\omega = 35000$ ev to $\omega \rightarrow \infty$, with the constant A obtained by fitting this function to the data from the tables at $\omega = 35000$ ev.

Using this data, eq. (5) for $n(\omega_o)$ was numerically evaluated at 378 points ω_o in the range 0.15 ev to 30000 ev; the trapezoidal rule was used, and the intervals were taken smaller in the energy range where there is structure in $\kappa(\omega)$. The values of $n(\omega_o)$ and

$\kappa(\omega_0)$ at the 378 points are then used to calculate $R(\omega_0)$, $\theta(\omega_0)$, $\varepsilon_1(\omega_0)$ and $\varepsilon_2(\omega_0)$ at these points. using eqs. (6). We note that we have ignored absorption by the lattice in the far infra-red ($\simeq$ .04 to .60 ev); this small effect, which involves multiple phonon processes, should not have an appreciable effect on the optical properties at higher energies.

In the next step we compiled a set of data for $R(\omega)$ for the full spectrum. For low energies. up to 1.5 ev, we used the $n(\omega)$ measurement of Primak[19], Schwidefsky[20], and Villa[21]. In this region, where $\kappa(\omega) \simeq 0$, $R(\omega)$ is simply obtained from $n(\omega)$ by the expression,

$$R(\omega) \simeq \frac{(n(\omega) - 1)^2}{(n(\omega) + 1)^2} . \tag{9}$$

From 1.5 ev to 10 ev we used the reflectivity measurements of Verleur[22]. For $\omega > 10$ ev, the $R(\omega)$ results from our calculation above were used up to 30000 ev, and the free electron behavior, $R(\omega) \propto \omega^{-4}$, was used for the high energy extrapolation. We numerically integrated eq. (4) for the same 378 points ω_0 as above, and subsequently calculated a new set of values for $n(\omega_0)$, $\kappa(\omega_0)$, $\varepsilon_1(\omega_0)$. and $\varepsilon_2(\omega_0)$.

To continue, we compiled an improved set of $\kappa(\omega)$ data, using the earlier choice up to 3.0 ev, the results from the $R(\omega)$ to $\theta(\omega)$ calculation just above for the range 3.0 ev to 10 ev. and the earlier choice of $\kappa(\omega)$ for $\omega > 10$ ev; this data is shown in

Figs. 1,2, and 3 (Fig. 2 shows $\kappa(\omega)$ only in the important visible and ultraviolet regions and Fig 3 shows the low energy region; various experimental points are included). The large absorption in the visible and ultraviolet, including the peaks near 3.4, 4.3, and 5.5 ev, are due to electronic transitions from the valence to the conduction band. the increases in absorption at 100 ev and at 1840 ev are due to L-shell and K-shell core excitations, respectively. Integrating eq. (5) for this data produced the results shown in Figs. 4, 7, 9, and 10 for $n(\omega)$, $R(\omega)$, $\varepsilon_1(\omega)$, and $\varepsilon_2(\omega)$ respectively. Figs. 5 and 6, and 8 show $n(\omega)$ and $R(\omega)$, respectively, in restricted energy regions, and include various experimental values. In addition, we have included the energy loss function, $-\text{Im}(1/\varepsilon(\omega))$, Fig. 11; this function shows a peak at the bulk plasmon frequency of 16.7 ev.

As we will discuss in the next section, these results obey the sum rules very well. The values we obtain for $n(\omega)$ and $\varepsilon_1(\omega)$ at the very low energies are within one percent of the experimental results, which is within the accuracy expected from the numerical integrations (see Fig. 5 for the $n(\omega)$ comparision, where our data is given by the solid curve; also, we obtain $\varepsilon_1(o) \simeq 11.5$). We note here that the iterations and data choice described above were not the only ones that we examined; we initially used the Philipp[2] reflectivity data in the band-to-band region, and also the Philipp and Taft[9] data in the same region, but in both cases were unable, after several iterations, to reproduce the experimental values for n and ε_1 at low energies, obtaining values 6%

to 9% too small, as shown by the dashed curve in figure 5 for n (the illustrated case utilizes ref. 2 reflectivity from 1.6 to 5.4 ev). It seems that the reflectivity values of references 2 and 9 are too small; the Verleur[22] data appears to correct this problem. The Philipp and Taft reflectivity data was obtained from samples that may have been contaminated by oxides. The Verleur data, and our results, will be discussed further in section 4.

We note here that only the graphs of our results are presented in this paper. Tables will be published elsewhere.

3. SUM RULES

We first consider the inertial sum rule[4] of eq. (7), which states that the average value of the index of refraction $n(\omega)$ is unity. It is convenient to define a verification parameter ζ by dividing by the absolute sum,

$$\zeta = \frac{\int_0^\infty (n(\omega) - 1) d\omega}{\int_0^\infty |n(\omega) - 1| d\omega} .$$

Due to uncertainities in the calculations, particularly in the numerical evaluation of this and the Kramers-Kronig integral, a calculated value of a few hundredths for ζ should indicate good agreement.

We obtain, utilizing our calculated $n(\omega)$ for the range 0.15 ev $\leq \omega \leq 30000$ ev, $n(\omega)$ = constant for $\omega < 0.15$ ev, and free electron behavior $n(\omega) \approx 1 - B/\omega^2$ for $\omega > 30000$ ev where B is a constant determined by fitting the data at $\omega = 30000$ ev,

$$\zeta \simeq - .0015,$$

which is an excellent result and shows consistency in our calculation.

The f-sum rules, which as mentioned earlier may be written in three formally distinct forms for the analysis of optical spectra, give the number of electrons (per atom if suitably normalized) effective in dissipative processes.

$$\int_0^\infty \omega \varepsilon_2(\omega)\, d\omega = \frac{\pi}{2}\, \omega_p^2 \,, \tag{10a}$$

$$\int_0^\infty \omega \kappa(\omega)\, d\omega = \frac{\pi}{4}\, \omega_p^2 \,, \tag{10b}$$

$$\int_0^\infty \omega \operatorname{Im}\left[\tilde{\varepsilon}^{-1}(\omega)\right] d\omega = -\frac{\pi}{2}\, \omega_p^2 \,, \tag{10c}$$

where $\omega_p = (4\pi N e^2/m)^{\frac{1}{2}}$, N denoting the electron density, is the plasma frequency. It is useful to define the effective number of electrons contributing to the optical properties up to an energy ω' by the partical f-sums (constant C is as given below eq. (8)),

$$n_{eff,\varepsilon_2}(\omega') = C \int_0^{\omega'} \omega \varepsilon_2(\omega)\, d\omega, \tag{11a}$$

$$n_{eff,\kappa}(\omega') = 2C \int_0^{\omega'} \omega \kappa(\omega)\, d\omega, \tag{11b}$$

$$n_{eff,\varepsilon^{-1}}(\omega') = -C \int_0^{\omega'} \omega \operatorname{Im}\left[\tilde{\varepsilon}^{-1}(\omega)\right] d\omega. \tag{11c}$$

For $\omega' \to \infty$, we expect $n_{eff} = 14$ (per atom) for all three rules in silicon; but the three rules do not give the same value for the partial f-sums, that is, they differ significantly as a function of energy ω', essentially describing somewhat different processes[3].

The solid curves of Fig. 12 shows our results for n_{eff} as function of maximum energy ω'. We took $\varepsilon_2(\omega)$, $\kappa(\omega)$, and $-\text{Im}\left[\tilde{\varepsilon}^{-1}(\omega)\right]$ equal to zero for $\omega < 0.15$ ev and proportional to ω^{-4} for $\omega > 30000$ ev, and numerically integrated eqs. (11a, b, c) by the trapezoidal rule. The value for the ε_2 - sum just below the onset of L-shell excitations ($\omega' \simeq 100$ ev) is consistent with the value $n_{eff} \simeq 4.15$ predicted for the four valence electrons of silicon, when Pauli redistribution of oscillator strength is considered. Also, at this point, the three values of n_{eff} are in the proper order, the ε_2 - sum being larger than the κ - sum, which is itself larger than the $-\text{Im}\left[\tilde{\varepsilon}^{-1}\right]$ - sum; they are also in the proper ratio (from the graph we have values 4.15, 4.13, and 4.05). This ordering and ratio can be shown to be correct when the background effect of the core electrons is considered[3].

These three partial sum rules were also evaluated below the L-edge for the oxide-free data of Philipp[2], and these results are shown by the dashed curves on Fig. 12. They do not maintain the correct order, crossing at approximately 50 ev, showing that there is erroneous data below this energy.

Fig. 12 also shows the contribution to n_{eff} from the core electrons, as well the total contribution. We find that, as $\omega' \to \infty$ $n_{eff} \to \simeq 13.99$ electrons per atom, which is an excellent result considering the numerical integrations involved in the calculations. Considering the L-shell and the K-shell separately, they contribute, respectively, about 8.15 electrons and 1.68 electrons. Oscillator strength calculations, utilizing Hartree-Fock-Slater wave functions (using the Herman and Skillman program[23]) and con-

sidering Pauli redistribution of oscillator strength, predicts
8.33 for the eight L-electrons and 1.52 for the two K-electrons.
We feel that there is satisfactory agreement between our results
and the theory for these core electrons, when one considers the
errors inherent in utilizing the HFS atomic wave functions; we
note that the requirement of 14 electrons for the total sum must
be satisfied more closely than these partial sums.

4. DISCUSSION

As has been discussed above, our results for the optical
constants of silicon appear to be valid; both the sum rules and
the comparison with various experimental data are satisfied to
within computational accuracy. But some questions still arise
concerning the experimental data in the important range 3.0 ev
to 10 ev (we used the reflectivity data of Verleur[22] in this
range). A private communication revealed that the measurements
were made primarily to obtain data with which to illustrate
a theoretical method, rather than to make very accurate measure-
ments. Dr. Verleur has long since gone on to other work, and
commented mainly from memory; thus we do not really know the
accuracy of this data. New measurements of reflectivity and/or
dielectric function in this region could help to confirm or cor-
rect our results. Experimental measurements in the range 20 ev
to 95 ev, where we were unable to find any data, would also be
helpful.

Related to the f-sum rules is the expression for the loga-
rithmic mean excitation energy.

$$\ln I = \frac{\int_0^\infty \omega \ln(\omega) \; \text{Im}\left[\tilde{\epsilon}^{-1}(\omega)\right] d\omega}{\int_0^\infty \omega \; \text{Im}\left[\tilde{\epsilon}^{-1}(\omega)\right] \; d\omega} \; . \qquad (12)$$

This is particularly useful in that I may be obtained from other than optical experiments. For example, Tschalar and Bichsel[24] obtained I = 173.5 ev for silicon by fitting theoretical range functions to experimental energy loss data. Our data gives I = 166.7 ev, 3.9% smaller than the Tschalar and Bichsel result, using a high energy extrapolation of ω^{-4} (for $\omega > 30,000$ ev) in the integrals of eq. (12). Other extrapolations, for example, $\omega^{-3.9}$ and ω^{-3}, increase our result by only a very small amount. The data in the band-to-band region appears to have only a very small effect on the result for I. Small changes in extinction coefficient κ in the region from K-edge to 30,000 ev, where we used the tabulated κ data, have a large effect on the result for I.

Our calculations concern only pure silicon at 300°K. Due to the technical interest, we plan to extend the study to doped silicon, and to other temperatures. We expect an increase in absorption in the infrared with doping; in the n-type crystal, this is due to an increase in the number of charge carriers in the conduction band, and in the p-type crystals, to the increase in the number of holes in the valence band, hence available final states for low energy absorption. A decrease in the size of the energy gap with doping may also contribute to the change. The infrared absorption data of Schumann, et al[25] and of Fistul[26] show this expected increase. This increase in oscillator strength

in the infrared requires a decrease elsewhere; the result is a decrease in reflectivity in the band-to-band region, as can be seen in the doped silicon measurements of Lukes and Schmidt[27], Dubrovskii and Subashiev[28], and Bramer, et al[29]. This decrease may be explained, in the n-type crystals, by a decrease in the number of available final states in the conduction band, and in the p-type crystals by a decrease in the number of electrons occupying initial states in the valence band.

We expect little change in the optical constants with doping at energies above that at which the valence electrons are nearly saturated, as in this region the absorption is essentially that of the core electrons, overlying only a relatively weak continuum due to transitions from the valence band to higher levels in the conduction band. Some absorption due to the core levels of the dopant atoms will be present, but at the concentrations of interest will contribute very little. Brown, et al[11], shows only a slight changes in the shape of the absorption curve of n-type silicon when comparing the lightly and heavily doped results; they state that their other doped samples yielded absorption curves that could not be distinguished from that of intrinsic silicon.

We expect the absorption to decrease with decreasing temperature in the infrared, due to the decrease in the number of thermally excited electrons in the conduction band and holes in the valence band (and may also be due to an increase in the energy gap with decreasing temperature); this decrease in absorption is shown in the results of Dash and Newman[6], who measured absorption in pure single crystal silicon at $77^\circ K$ and $300^\circ K$.

The work of Lukes and Schmidt[27] indicates that reflectivity
is increased in the ultraviolet with a decrease in temperature.
This effect can be explained, similar but opposite to the
doped crystal discussion above, by a shift in oscillator
strength away from the infra red. For energies above the
L-edge, Gahwiller and Brown[11] observe little change in the
absorption spectrum of silicon upon cooling to 77°K. We
expect little temperature dependence in the optical constants
at X-ray energies, as, again, the optical effects there are
primarily due to the core levels.

REFERENCES

1. Philipp, H.R., and Ehrenreich, H., J. Appl. Phys., Vol. 35 1416 (1964).

2. Philipp, H.R., J. Appl. Phys., Vol. 43, No. 6, 2835 (1972).

3. Smith, D.Y. and Shiles, E., Bull. Am. Phys. Soc., 22, 92 (1977) and Phys. Rev. B, 17 , 4689 (1978).

4. Altarelli, M., Dexter, D.L., Nussensveig, H.M. and Smith, D.Y. Phys. Rev. B, Vol. 6, No. 12, 4502 (1972).

5. Shiles, E., and Smith, D.Y., Bull. Am. Phys. Soc., 22, 92 (February, 1977) and to be published.

6. Dash, W.C., and Newman, R., Phys. Rev., Vol. 99, No. 4, 1151 (1955).

7. So, S.S., and Vedam, K., J. Opt. Soc. Amer., Vol. 62, 16 (1972); So, S.S., and Vedam, K., J. Opt. Soc. Amer., Vol. 62 596 (1972).

8. Azzam, R.M.A., Zaghloul, A.-R.M., and Bashara, N.M., J. Opt. Soc. Amer., Vol. 65, No. 12, 1964 (1975).

9. Philipp, H.R., and Taft, E.A., Phys. Rev., Vol. 120, No. 1, 37 (1960).

10. Sasaki, T., and Ishiguro, K., Phys. Rev., Vol. 127, No. 4, 1091 (1962).

11. Brown, F.C., Bachrach, R.Z., and Skibowski, M., Phys. Rev. B, Vol 15, No. 10, 4781 (1977); Gahwiller, C., and Brown, F.C., Phys. Rev. B, Vol. 2, No. 6, 1918 (1970).

12. Hubbell, J.H., McMaster, W.H., Kerr Del Grande, N., and Mallett, J.H., in International Tables for X-Ray Crystallography, p. 47 (Publ. for the International Union of Crystallography by the Kynoch Press, Birmingham, England, 1974).

13. Storm, E., and Israel, H.I., University of California, Report LA 3753 (1967).

14. Henke, B.L., Elgin, R.L., Lent, R.E., and Ledingham, R.B., Norelco Reporter, Vol. 14, Nos. 3-4, p. 112 (1967).

15. Henke, B.L., and Ebisu, E.S., in Advances in X-Ray Analysis, Vol. 17, ed. by C.L. Grant, C.S. Barrett, J.B. Newkirk, and C.O. Ruud, p. 152 (Plenum Press, New York, 1973; Conference held Aug 1973).

16. Bracewell, B.L., and Veigele, W.J., in Advances in X-Ray Analysis, Vol 15, ed. by K.F.J. Heinrich, C.S. Barrett, J.B. Newkirk, and C.O. Ruud, p. 352 (Plenum Press, New York, 1972; conference held Aug. 1971).

17. Compton, A.H., and Allison, S.K., X-Rays in Theory and Experiment, Second Edition, p. 802 (D. Van Nostrand Co. Inc., 1935).

18. McGinnies, R.T., Supplement to NBS Circular 583 (1959).

19. Primak, W., Appl. Optics, Vol. 10, No. 4, 759 (1971).

20. Schwidefsky, F., Thin Solid Films, 18, 45 (1973).

21. Villa, John J., Appl. Optics, Vol. 11, No. 9, 2102 (1972).

22. Verleur, H.W., J. Opt. Soc. Amer., Vol. 58, No. 10, 1356 (1968).

23. Herman, F., and Skillman, S., Atomic Structure Calculations (Prentice-Hall, Inc., Englewood Cliffs, N.J., 1963).

24. Tschalar, C., and Bichsel, H., Phys. Rev., Vol. 175, No. 2, 476 (1968).

25. Schumann, P.A., Jr., Keenan, W.A., Tong, A.H., Gegenworth, H.H., and Schneider, C.P., J. Electrochem. Soc., Vol. 118, No. 1, 145 (1971).

26. Fistul, V.I., Heavily Doped Semiconductors, (Plenum Press, New York, 1969).

27. Lukes, F., and Schmidt, E., Proceedings of the 7th International Conference on the Physics of Semiconductors, p. 197 (1964).

28. Dubrovskii, G.B., and Subashiev, V.K., Sov. Phys.-Solid State, Vol. 5, No. 4, 805 (1963).

29. Bramer, B.R., Vertogen, G., and Penning, P., Solid State Commun., Vol. 1, 138 (1963).

FIGURE CAPTIONS

Fig. 1.　Extinction coefficient κ, as function of incident photon energy, for full range of optical electronic excitations.

Fig. 2.　Extinction coefficient κ, emphasizing the region of band-to-band transitions. Experimental results, from a smooth curve fit to the data of Sasaki and Ishiguro[10], are shown.

Fig. 3.　Extinction coefficient κ, for the low energy region. The experimental data shown are obtained from Azzam, et al[8], So and Vedam[7], Dash and Newman[6], and a smooth curve fitting the measurements of Philipp[2].

Fig. 4.　Index of refraction n, as function of incident photon energy, for the full range of optical electronic excitations.

Fig. 5.　Index of refraction n for the low energy region. The solid curve represents the result of the present calculation and the dashed curve a preliminary calculation using some of the reflectivity data of reference 2 (see text). The experimental data shown are that of Azzam, et al[8], So and Vedam[7], Villa[21], Primak[19], and a smooth curve fitting the data of Schwidefsky[20].

Fig. 6.　Index of refraction n, emphasizing the region of band-to-band transitions. The experimental data shown are that of Azzam, et al[8], So and Vedam[7], and a smooth curve fit to the data of Sasaki and Ishiguro[10].

Fig. 7.   Reflectivity R, as function of incident photon energy, for the full range of optical electronic excitations.

Fig. 8.   Reflectivity R, emphasizing the region of band-to-band transitions. The solid curve represents the result of the present calculation and the dotted curve is a smooth fit to the reflectivity measurements of Philipp and Taft[9]. The experimental measurements of Verleur[22] are shown; we note that we started with Verleur's data in the region shown, but that the solid curve is the result after a full Kramers-Kronig iteration.

Fig. 9.   Real part of the dielectric function, ε_1, as a function of photon energy, for the full range of optical electronic excitations.

Fig. 10.   Imaginary part of the dielectric function, ε_2, as a function of photon energy, for the full range of optical electronic excitations.

Fig. 11.   Energy loss function, $-\mathrm{Im}\left[\tilde{\varepsilon}^{-1}\right]$, illustrating the peak at the bulk plasmon frequency of 16.7 ev.

Fig. 12.   Number of electrons per atom contributing to the optical properties, as a function of upper limit of integration, calculated from the three forms of the f-sum rule. The solid curves show the results using the data from the present calculation, and the dashed curves using the data from reference 2. The onset of core electron excitations are indicated.

Fig. 1

Fig. 2

Fig. 3

Fig. 4

Fig. 5

+ Reference 8
× Reference 7
● Reference 21
◐ Reference 19
◑ Reference 20

Fig. 6

Fig. 7

Fig. 8

O Reference 22

R

1.0

0.5

0

10

20

ω(ev.)

Fig. 9

Fig. 10

Fig. 11
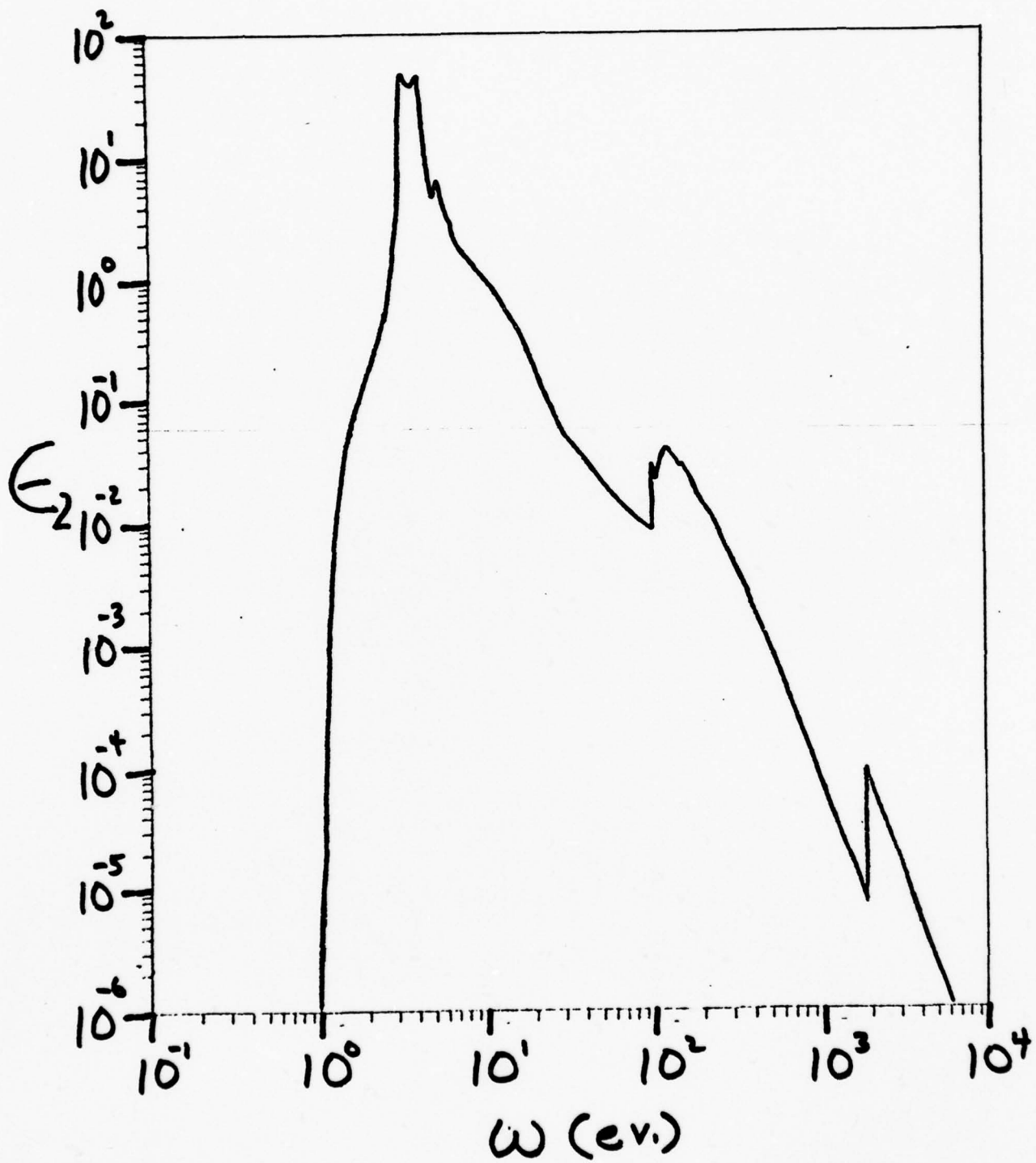

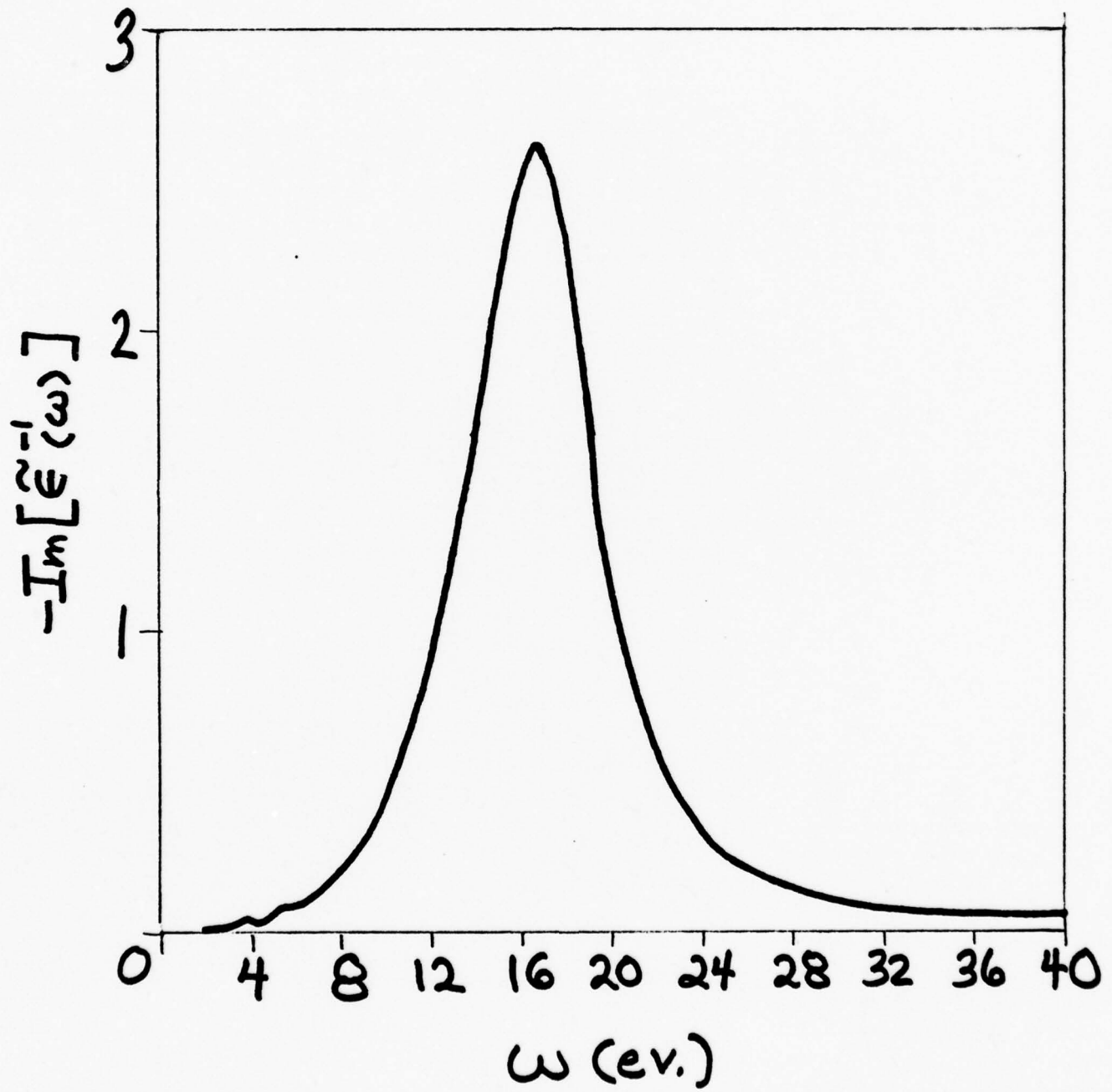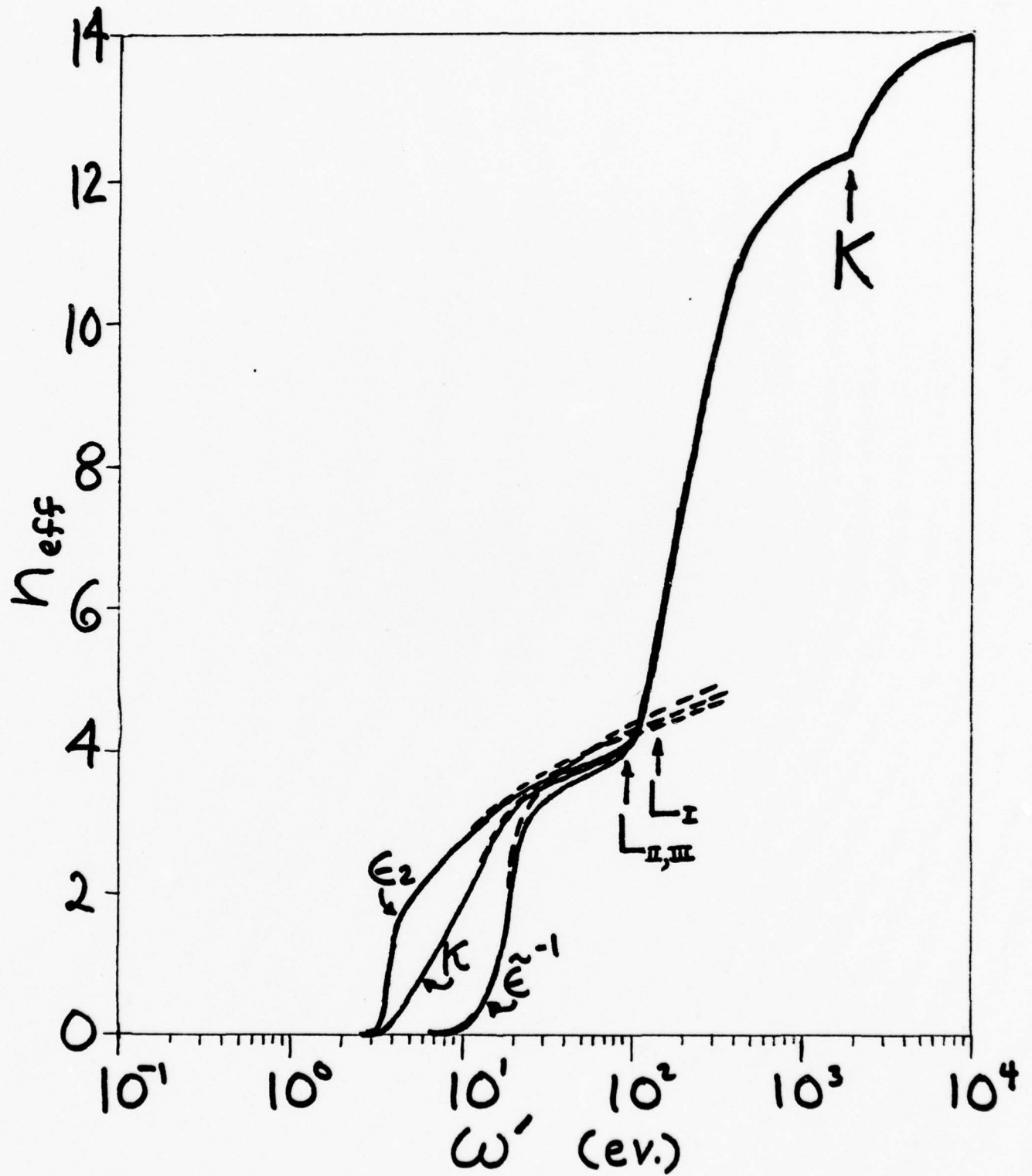$-Im[\tilde{\epsilon}^{-1}(\omega)]$ vs. ω (ev.)
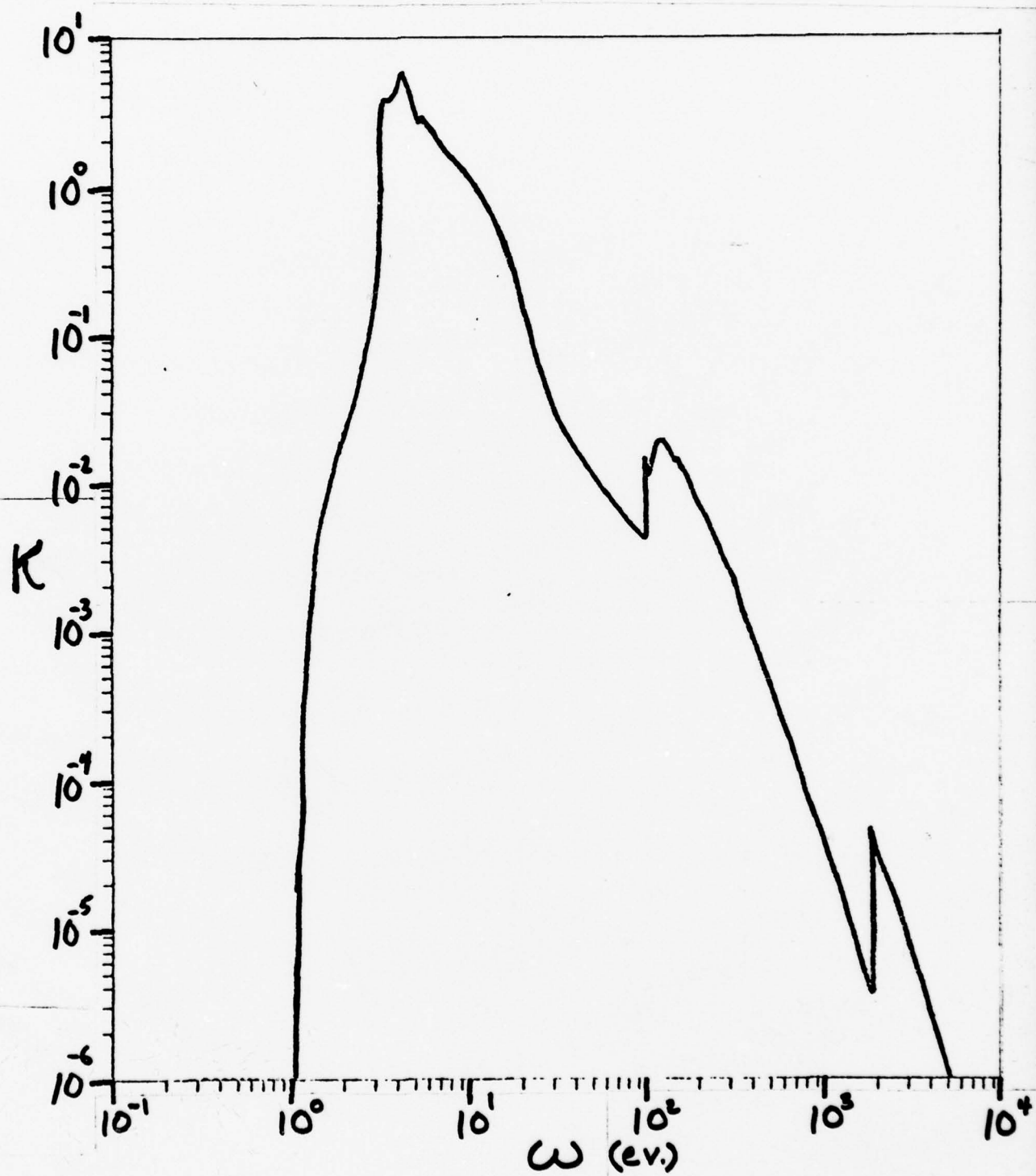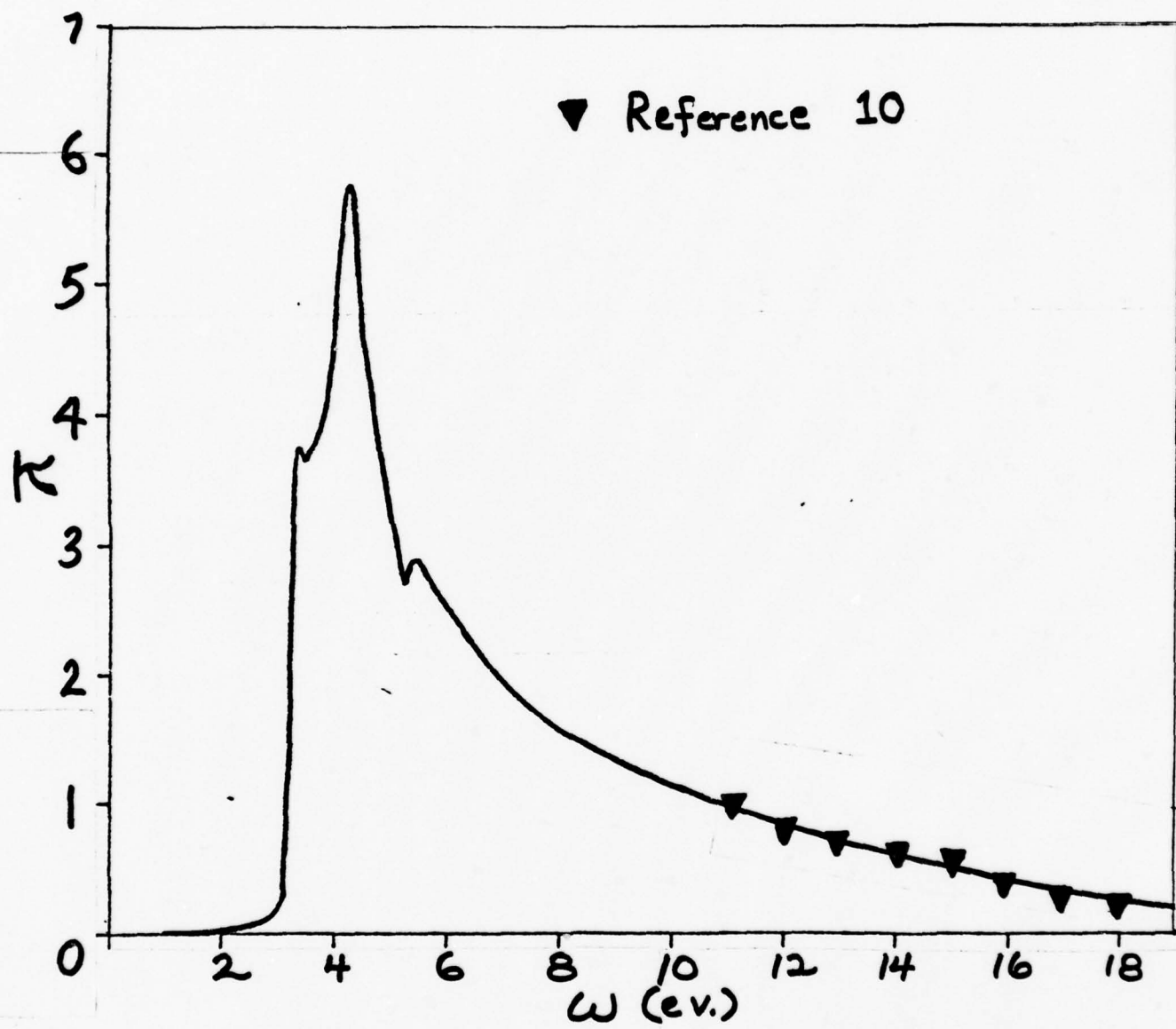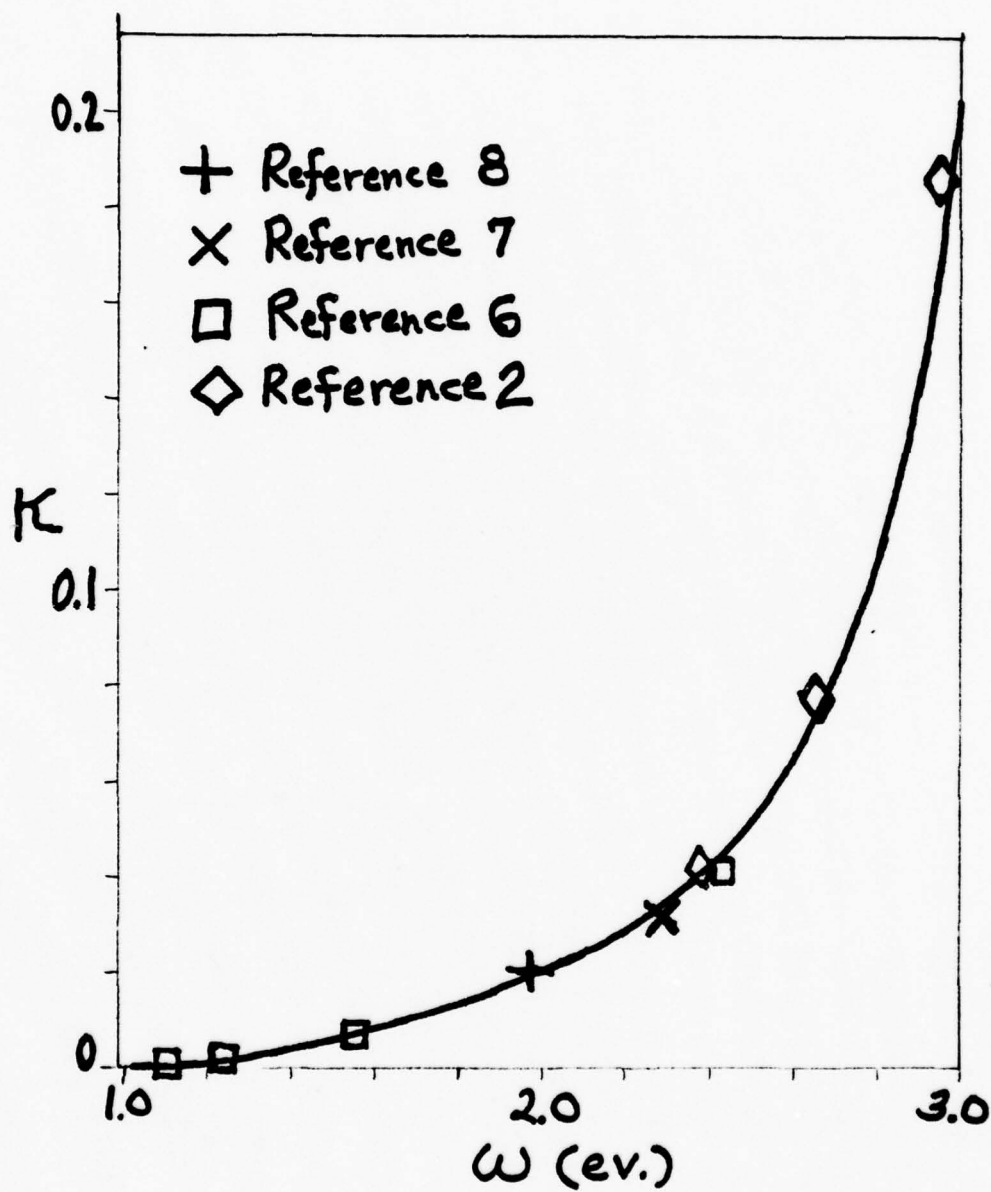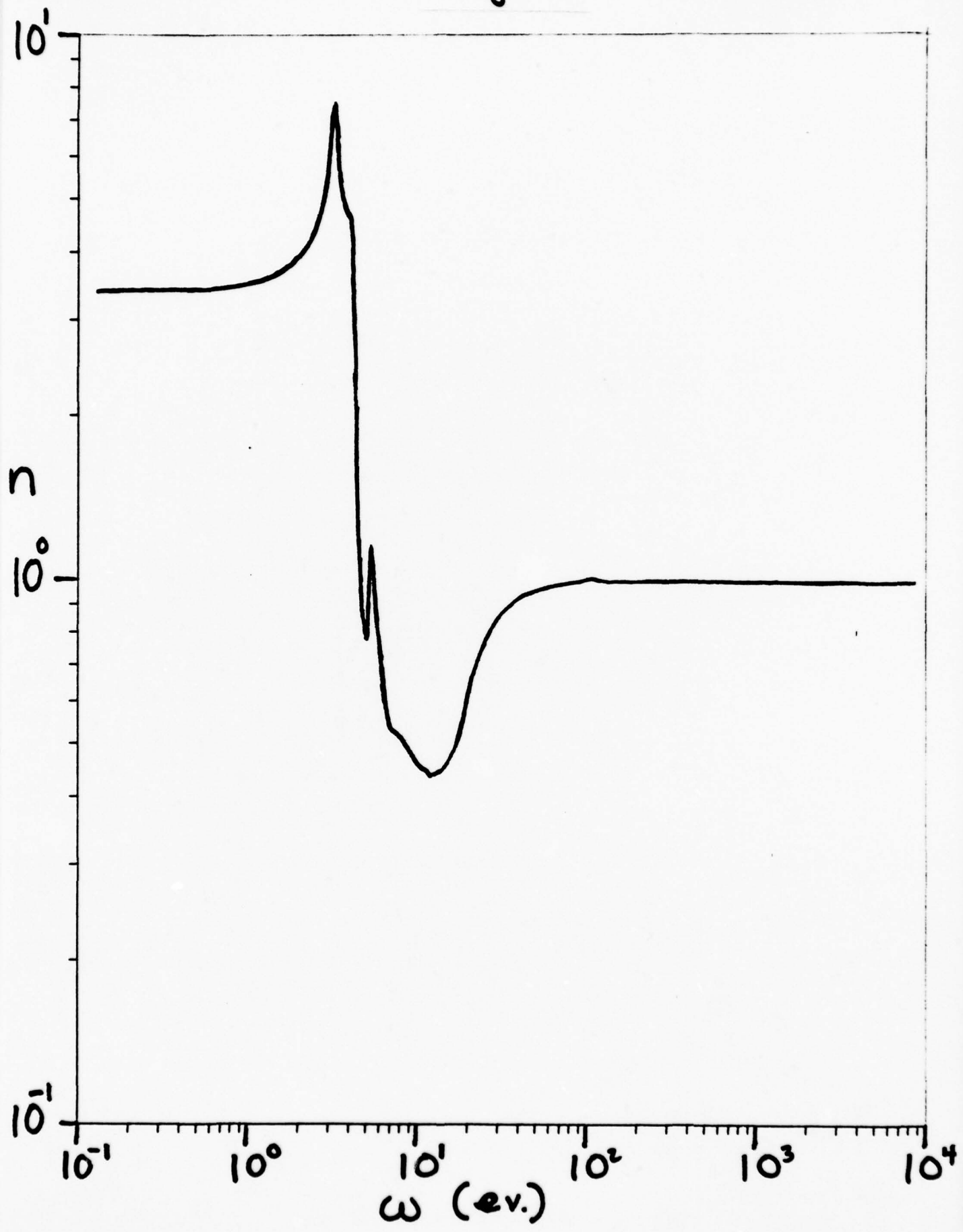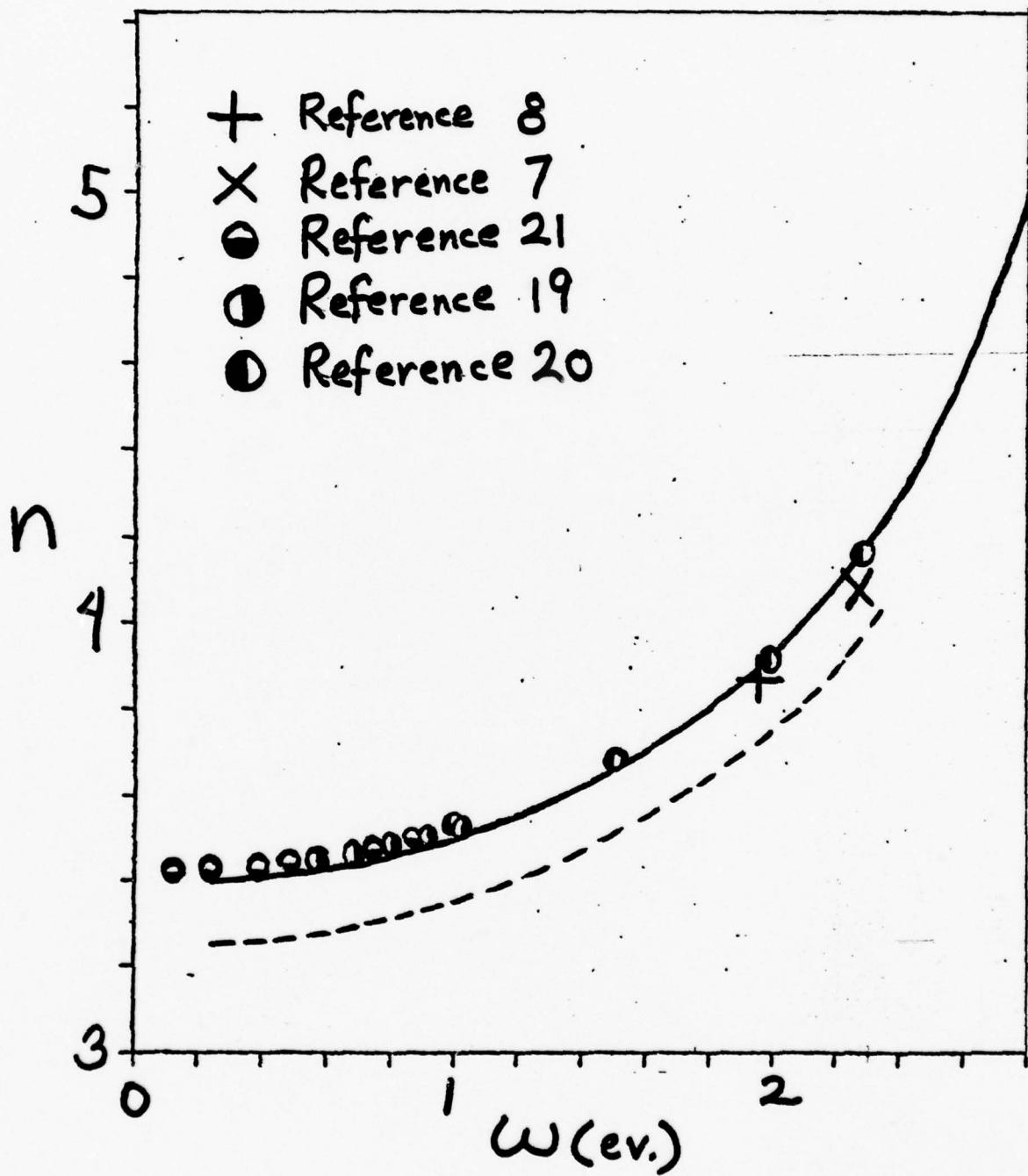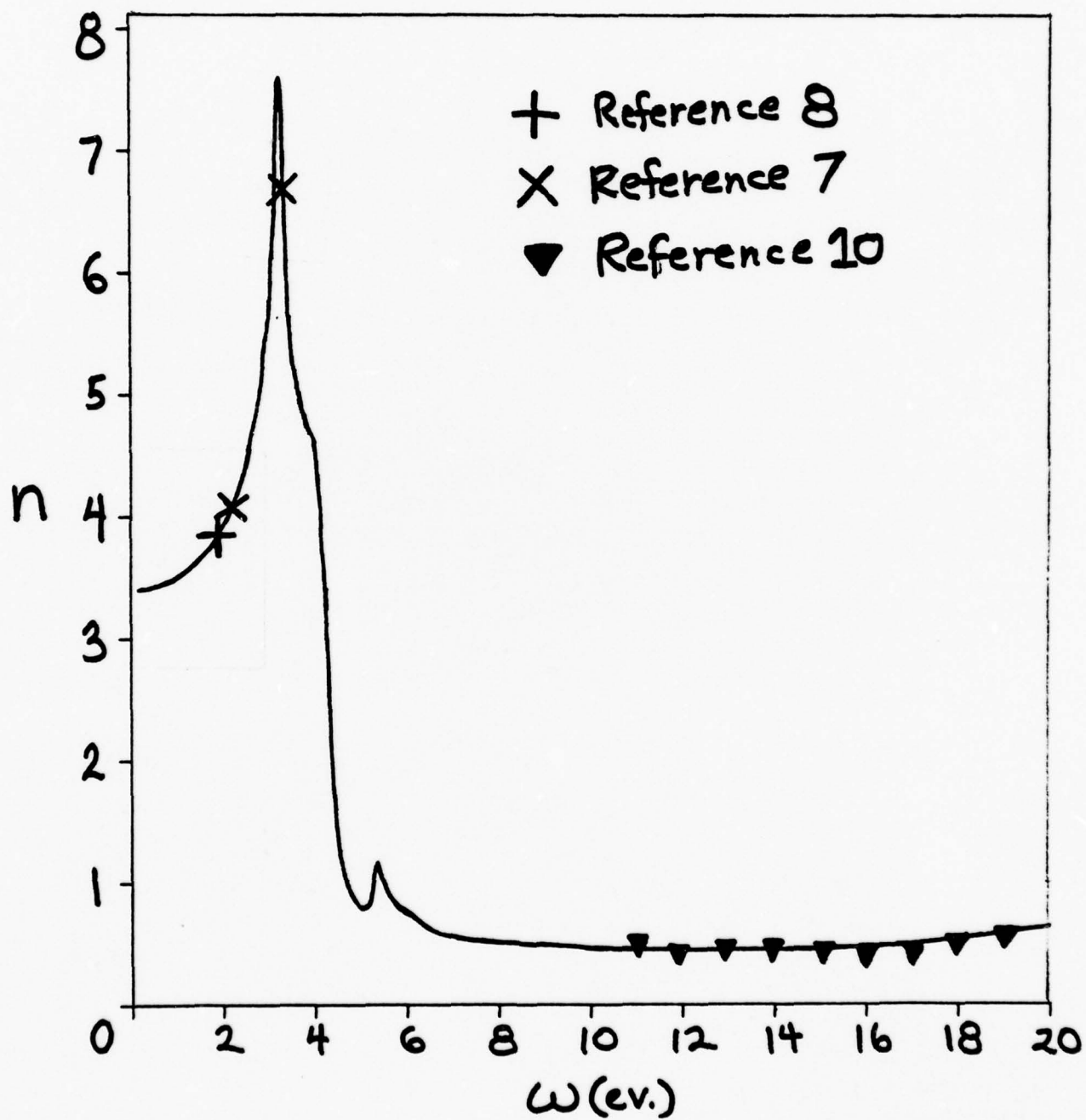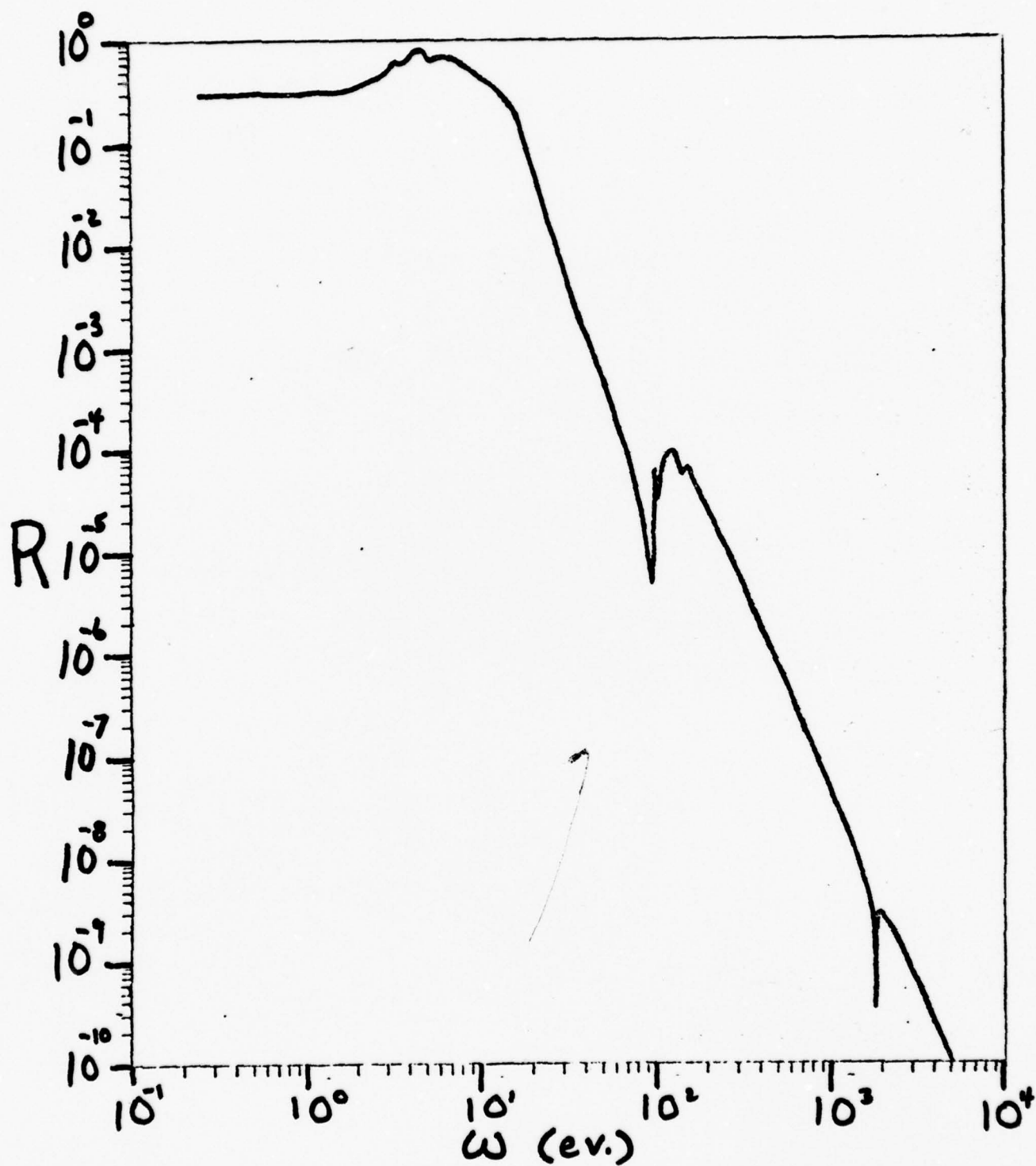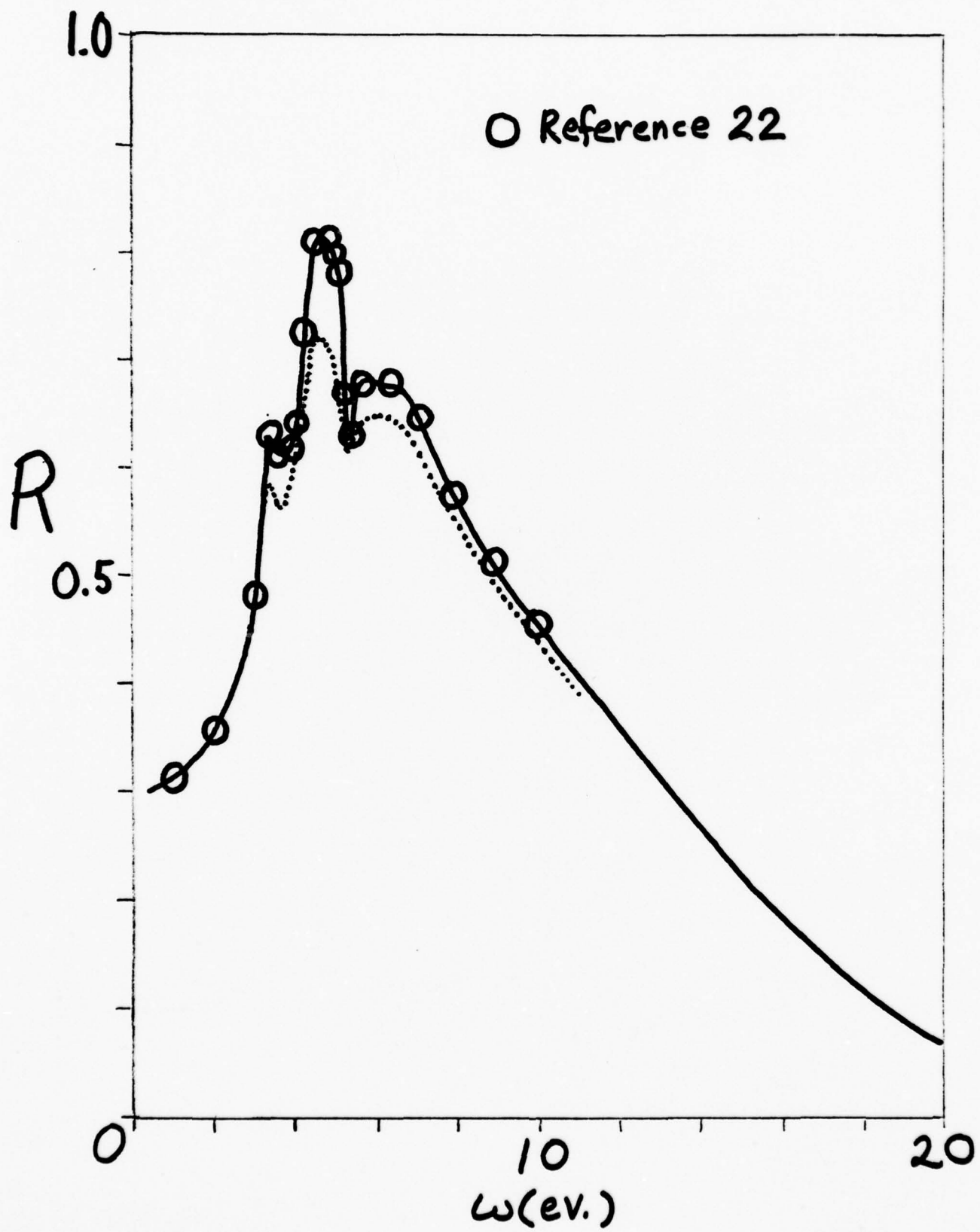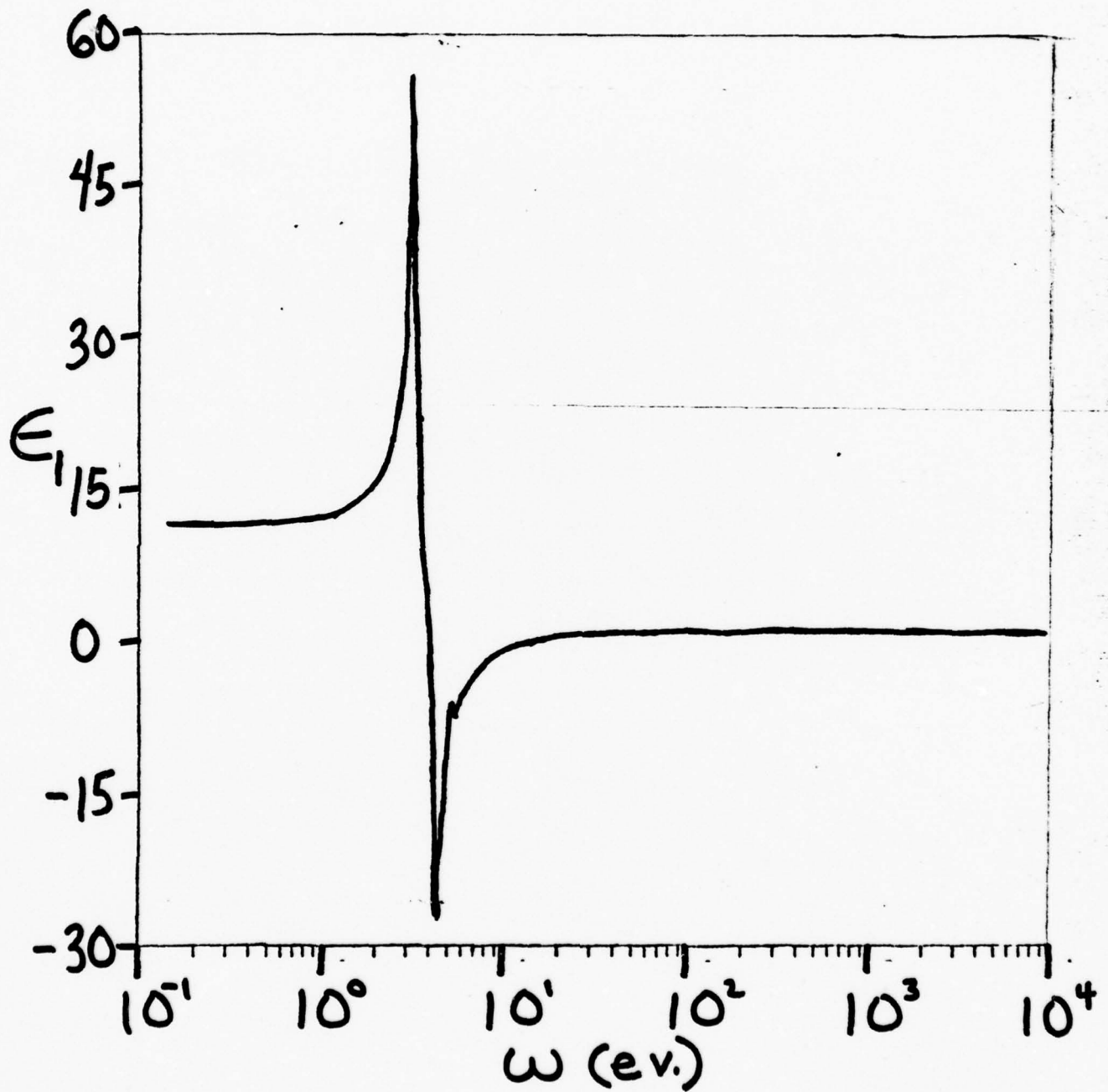
Fig. 12

(Optical Constants of Gallium Arsenide)

1. INTRODUCTION

We have performed a Kramers-Kronig analysis of the available experimental measurements of the optical constants of the III-V semiconductor Gallium Arsenide. Only pure material, at 300°K. was considered. Various sum rules were used to evaluate the self-consistency of our calculation and the accuracy of the experimental data. Our results include the full range of optical electronic excitations, from the infrared to X-rays.

Absorption by optical phonons in the far infrared is ignored in the basic calculation; these effects, although large in an ionic material such as GaAs, do not appreciably affect the Kramers-Kronig analysis in the electronic absorption region and do not significantly affect the sum rules analysis. For completeness we have examined briefly the experimental measurements, by Piriou and Cabannes[1], of the reflectivity in GaAs in the phonon region.

Absorption data in the X-ray region for photon energies above 158 ev were not available, and we approximated the extinction co-efficient from 158 ev to 45000 ev by an appropriate combination of X-ray data on Gallium and Arsenic. This should provide a reasonable approximation, since the electronic excitations at these high energies involve primarily the core electrons.

As will be discussed below, our results indicate that the reflectivity measurements in the band-to-band region may be too small, and that the approximation in the X-ray region, while reasonable, results in a total oscillator strength there that is too small - this may be

due to incomplete data (on Ga and As) at low X-ray energies
near the M_I core levels, and at energies just above the onset of
L-shell excitations.

Section 2 presents the choice of experimental data, the com-
putation method, and the results, while section 3 gives the sum
rules analysis and section 4 a brief discussion of the region of
optical phonon absorption. Section 5 contains a discussion of
the results.

2. KRAMERS-KRONIG ANALYSIS

The Kramers-Kronig integral that enables one to calculate
index of refraction $n(\omega_0)$ of material at incident photon energy
ω_0 from extinction coefficient $\kappa(\omega)$ is

$$n(\omega_0) = 1 + \frac{2}{\pi} P \int_0^\infty \frac{\omega \kappa(\omega) d\omega}{\omega^2 - \omega_0^2} \tag{1}$$

where P indicates that the principal value is to be taken. Thus
to produce $n(\omega_0)$, $\kappa(\omega)$ must be known at all energies ω. When
this analysis can be made at a chosen energy ω_0, the other
optical constants such as the normal incidence reflectivity
$R(\omega_0)$, phase shift $\Theta(\omega_0)$, and real and imaginary parts of the
dielectric funtion $\varepsilon_1(\omega_0)$ and $\varepsilon_2(\omega_0)$ (in the limit of long
wavelength, and in materials where the dielectric response is
isotropic, where the dielectric properties can be described
by the complex dielectric function involving only these two
numbers) may be evaluated from the expressions

$$R(\omega_0) = \frac{(n(\omega_0) - 1)^2 + \kappa(\omega_0)^2}{(n(\omega_0) + 1)^2 + \kappa(\omega_0)^2} \quad ,$$

$$\tan \theta(\omega_0) = \frac{-2\kappa(\omega_0)}{n(\omega_0)^2 + \kappa(\omega_0)^2 - 1} \quad ,$$

$$\epsilon_1(\omega_0) = n(\omega_0)^2 - \kappa(\omega_0)^2 \quad ,$$

$$\epsilon_2(\omega_0) = 2n(\omega_0)\kappa(\omega_0) .$$

$$(2)$$

Similarly, if $R(\omega)$ is known for all incident photon energies from 0 to ∞, then $\theta(\omega_0)$ can be evaluated from the Kramers-Kronig integral,

$$\theta(\omega_0) = \frac{\omega_0}{\pi} P \int_0^\infty \frac{\ln R(\omega)\, d\omega}{\omega^2 - \omega_0^2} . \tag{3}$$

The other constants can then be found at a chosen energy ω_0 by various combinations of equations (2).

Since absorption data was available for both high and low energies for the semiconductor GaAs (but not in the region of band-to-band transitions), we chose to construct a full set of extinction coefficient data to begin the analysis. For very small energies (below 1.375 ev) we choose $\kappa(\omega) = 0$; this behavior is due to the scarcity of electrons in the conduction band and holes in the valence band in pure GaAs at 300°K. Experiments[1,2] show appreciable phonon absorption below .04 ev, but this effect

does not contribute importantly to the Kramers-Kronig integral for ω_0 in the electronic absorption region and it was thus neglected in our basic calculation; some discussion of this phonon absorption is given later. Absorption data in the range 1.375 ev to 1.46 ev was obtained from the measurements of Sturge[3], and the range 1.46 ev to 2.7 ev was approximated. The results of a partial Kramers-Kronig analysis by Philipp and Ehrenreich[4] was used as an initial approximation in the band-to-band region, up to 17.0 ev. Cardona, et al[5], has measured the absorption in GaAs from 15.0 ev to 158 ev using a synchrotron source, and we used their data from 17.0 ev to 158 ev. Above 158 ev we were unable to obtain any absorption data for GaAs, and had to approximate by combining X-ray absorption data[6,7,8,9] for Ga and As - this should be a reasonable approximation since the atomic core electrons are primarily responsible for the absorption at these high energies. Thus, for the range 109 ev to 45000 ev (109 ev is the lowest point for which we had Ga and As X-ray data) we approximated extinction coefficient κ for GaAs from the expression

$$\kappa(\omega) \approx .434 \kappa_{Ga}(\omega) + .481 \kappa_{As}(\omega) ,$$

(4)

where .434 is the ratio of the number density of Ga atoms in GaAs as compared to the pure element and .481 is the same ratio for As (using mass densities of 5.32 gm/cm^3 for GaAs, 5.90 gm/cm^3 for Ga,

and 5.73 gm/cm^3 for As). In the region of overlap, expression (4), using the Ga and As absorption data, gives results about 8 percent smaller than the measurements of Cardona, et al; for our initial choice we approximated the region 158 ev to 450 ev by fitting value and slope to Cardona's data at 158 ev and to expression (4) at 450 ev. Extinction coefficient κ for the range 450 ev to 45000 ev was then obtained from eq (4), and we used the extrapolation $\kappa(\omega) \alpha \omega^{-4}$ for $\omega > 45000$ ev. We note that there was very little absorption data available for Ga and As in the region of onset of L-shell excitations (approximately 1000 ev to 1600 ev) and our initial construction of κ in this range is only a very rough approximation.

Using this data, eq. (1) for $n(\omega_0)$ was numerically evaluated at 367 points ω_0 in the range 0.30 ev to 40000 ev: the trapezoidal rule was used, and the intervals were taken smaller in the energy range where there is structure in $\kappa(\omega)$. $R(\omega_0)$, $\theta(\omega_0)$, $\varepsilon_1(\omega_0)$, and $\varepsilon_2(\omega_0)$ were then calculated using eqs. (2).

The next step in the iteration was to construct a full set of reflectivity $R(\omega)$ data, and then to use eqs. (2) and (3) to calculate a new set of extinction coefficient $\kappa(\omega)$ data; this step is required primarily to obtain an improved set of $\kappa(\omega)$ data in the band-to-band region, where reflectivity $R(\omega)$ can be accurately measured (and $\kappa(\omega)$ cannot). At low incident photon energy (approx. 0.73 ev to 1.38 ev) we used the index of refraction $n(\omega)$ data of Marple[10]; in this range, where $\kappa(\omega) \simeq 0$, $R(\omega)$ is obtained from $n(\omega)$ by

$$R(\omega) \approx \frac{(n(\omega)-1)^2}{(n(\omega)+1)^2} .$$

Below .73 ev, we assumed a smooth fit of the above data to $R(\omega=0) \simeq .2858$[15], again ignoring the effects of phonon absorption. For the band-to-band region, we used the reflectivity measurements of Philipp and Ehrenreich[4]; their data extended to about 25 ev, but we utilized it only up to 17.0 ev, choosing instead to rely on the Cardona absorption data above 17.0 ev, where reflectivity is small. We note that Philipp and Ehrenreich's reflectivity curve, while showing an increase in the region of d-band absorption (20-22 ev). does not show the double-peaked structure that Cardona, et al[5], in presenting their absorption data, associated with a double peak in the density of conduction states. From 17.0 ev to 45,000 ev, the $R(\omega)$ values resulting from the initial Kramers-Kronig integration above were used, and above 45000 ev, free electron behavior, $R(\omega) \alpha \omega^{-4}$, was assumed. We numerically integrated eq. (3) for the same 367 points ω_0 as above, and subsequently calculated a new set of values for $n(\omega_0)$, $\kappa(\omega_0)$, $\varepsilon_1(\omega_0)$, and $\varepsilon_2(\omega_0)$.

We were then able to compile an improved set of $\kappa(\omega)$ data, using the results of the $R(\omega)$ to $\theta(\omega)$ calculation in the band-to-band region and the earlier choice for $\kappa(\omega)$ above and below this region. Integrating eq. (1) for this improved $\kappa(\omega)$ then resulted in a new complete set of optical constants (again at 367 chosen points in the range 0.30 ev to 40,000 ev, including all of the important optical electronic excitations). We note that the full iteration was repeated several times, varying the approximations in

the regions 1.46 ev to 2.6 ev, 158 ev to 450 ev, and 1000 ev to 1600 ev, in order to obtain an optimum overall match to all the experiments and best satisfaction of the sum rules consistent with the experiments (discussed in the next section).

Figure 1 shows the improved set of $\kappa(\omega)$ data, for the full range considered. The large absorption in the range 1.4 ev to about 15 ev is due to electronic transitions from the valence to the conduction band. d-band absorptions are exhibited by the increases in absorption beginning at about 20 ev (Ga 3d electrons) and 41 ev (As 3d electrons). Absorption peaks due to $M_{II,III}$ levels appear just above 100 ev (Ga 3p electrons) and just above 140 ev (As 3p electrons); this structure is more evident in figure 2a. Additional M-core absorptions are also expected at about 158 ev (Ga 3s electrons) and 203 ev (As 3s electrons), but we did not find any data to give the associated structure in $\kappa(\omega)$ and had to approximate the region; these M_I levels are expected to contribute considerably less to the absorption than do the $M_{II,III}$ levels. Just above 1100 ev is the onset of the L - shell absorptions (Ga 2p and 2s electrons, and, at somewhat higher energies, the As 2p and 2s electrons); as can be seen in Figure 2b, very little data (on Ga and As) was available in this region, so the curve here is only a rough approximation with peaks assumed at the atomic energy levels of Ga and As. The onset of K shell absorptions are seen just above 10000 ev (Ga and As 1s electrons). As an aid in understanding the absorptions, Table I gives the energies of the various coure levels in the Ga and As atoms (taken from reference 11).

8.

Table I. ATOMIC ENERGY LEVELS[11]

(values are given in electron volts)

Gallium		Arsenic	
K	10,367	K	11,867
L_I	1298	L_I	1527
L_{II}	1142	L_{II}	1359
L_{III}	1115	L_{III}	1323
M_I	158.1	M_I	203.5
M_{II}	106.8	M_{II}	146.4
M_{III}	102.9	M_{III}	140.5

The solid curves in figures 2a,b, and c show $\kappa(\omega)$ in the X-ray region, and include the data that was used to define these curves, while figure 3 exhibits κ in the important band-to-band region, including some experimental data at the upper and lower ends of this range. Figure 4 gives κ near the absorption edge, and shows the data of Sturge[3] and of Panish and Casey[12].

In figure 5 we exhibit the normal incidence reflectivity curve resulting from our calculation; the structure is due to the various absorptions, as discussed above for extinction coefficient. Figure 6 shows our reflectivity results near the band edge, as well as experimental measurements of R and of index or refraction n(we can calculate $R \simeq \dfrac{(n-1)^2}{(n+1)^2}$ where κ is small). As will be discussed

below, our final Kramers-Kronig integration was unable to repro-
duce the experimental values at the low end (where $\kappa \cong 0$); this
is probably due to R values in the band-to-band region that are
too small, possibly due to oxides and/or surface preparation prob-
lems. Figure 7 exhibits R in the band-to-band region and the
experimental measurements of Philipp and Ehrenreich (points taken
from their published curve, which are not necessarily their data
points). We note that we used their data in this range but that our
final result (the solid curve) is the result of a full Kramers-
Kronig iteration (two numerical integrations). The dashed curve
in figure 7 was drawn to fit the R measurements of Morrison[13],
which extend to about 5.5 ev. In figure 8 we show reflectivity
from 15 ev to 24 ev, exhibiting the onset of d-band excitations.
We note that, as mentioned earlier, we used the absorption data
of Cardona, et al[5], at and above 17 ev, rather than the reflec-
tivity data of Philipp and Ehrenreich; the lack of a very close
match shows that the two sets of measurements are not fully
consistent with each other in the region 17 ev to 23 ev.

Figure 9 shows index of refraction $n(\omega)$ for the full range,
while figure 10 shows $n(\omega)$ at low energies, along with some
experimental data. The discrepancy between our results and
experiment at the low end is related to that discussed above for
reflectivity.

Figures 11 and 12 show, respectively, the real part ε_1 and
imaginary part ε_2 of the dielectric function for the full photon

energy range considered, while figure 13 exhibits the energy loss function $-\text{Im}\left[\tilde{\varepsilon}(\omega)^{-1}\right] = \varepsilon_2 / (\varepsilon_1^2 + \varepsilon_2^2)$. For the same reason as discussed above for reflectivity R, the ε_1 result cannnot be trusted at low energies. For example, one expects, from experiment, $\varepsilon_1 \simeq 13.10$ below the absorption edge; our result is clearly smaller than this.

Before proceeding with a further discussion of our results, we present an analysis of the various sum rules.

3. SUM RULES

The inertial sum rule[16] essentially tests the self-consistency of the index of refraction data, hence that of the other optical constants obtained in the same calculation.

$$\int_0^\infty (n(\omega)-1)\,d\omega = 0.$$

(5)

It is convenient to define a verification parameter ξ by dividing by the absolute sum,

$$\xi \equiv \frac{\int_0^\infty (n(\omega)-1)\,d\omega}{\int_0^\infty |n(\omega)-1|\,d\omega}.$$

Due to uncertainties in the numberical calculations (and in the experimental numbers used), a calculated value of a few hundredths for ξ should indicate good agreement.

We obtain $\xi \simeq -.0007$, which is an excellent result.

The f-sum rules may be written in three formally distinct forms for the analysis of optical spectra.

$$\int_0^\infty \omega F(\omega) \, d\omega = \frac{\pi}{2} \omega_p^2 , \qquad (6)$$

where $F(\omega)$ is one of the three expressions $\varepsilon_2(\omega)$, $2\kappa(\omega)$, or $-\text{Im}\left[\tilde{\varepsilon}(\omega)^{-1}\right]$. $\omega_p = (4\pi N e^2/m)^{\frac{1}{2}}$ is the plasma frequency, where N denotes electron density. These expressions may be normalized is such a way as to give number of electrons per atom or "molecule" contributing to dissipative processes. For our study of GaAs we obtain

$$n(\infty) = C \int_0^\infty \omega F(\omega) \, d\omega , \qquad (7)$$

where $C = .020846 \text{ ev}^{-2}$ for the GaAs "molecule". We expect a result $n(\infty) = 64$ for GaAs for all three f-sum rules; a result that is too small or too large indicates a lack of or an excess of oscillator strength, respectively, due to inaccuracies in the optical constants that form the integrand of eqn. (7).

One may also examine the distribution of oscillator strength by introducing the partial f-sums, where $n_{eff}(\omega')$ is the number of electrons contributing to the optical properties up to energy ω',

$$n_{eff,\epsilon_2}(\omega') = C \int_0^{\omega'} \omega \epsilon_2(\omega) \, d\omega, \tag{8a}$$

$$n_{eff,\kappa}(\omega') = 2C \int_0^{\omega'} \omega \kappa(\omega) \, d\omega, \tag{8b}$$

$$n_{eff,\epsilon^{-1}}(\omega') = -C \int_0^{\omega'} \omega \, Im[\tilde{\epsilon}^{-1}(\omega)] \, d\omega. \tag{8c}$$

The three rules do not give the same value for the partial sums, since the integrands describe somewhat different processes; they are expected to converge at large energies ω'.

The solid curves in Figure 14 exhibit the partial f-sums of eqs. (8a,b,c,) as a function of upper limit of integration ω'. At low energies ω' the three rules give results that differ substantially, and they are in the order $n_{eff,\epsilon_2} > n_{eff,\kappa} > n_{eff,\epsilon}-1$; this ordering can be shown to be correct when the background effect due to polarization of the core electrons is taken into account[17]. As ω' increases toward infinity, the three curves merge. We obtain $n(\infty) \simeq 62.55$ for all three rules, indicating a lack of oscillator strength as described by our data (as above, $n(\infty)$ should be 64). Further examination of the curves of Figure 14 can indicate the distribution of oscillator strength, hence help to locate the energy range(s) where the optical constants are inaccurate. As can be seen in Figure 14, the oscillator strength of the lower levels is not yet exhausted at the onset of

L-shell absorptions, and the oscillator strength of the L-shell is
not yet exhausted at the onset of K-shell absorptions. To obtain
a reasonable estimate of the oscillator strengths of the K-shell and
L-shell electrons (as described by our set of optical constants) we
first artificially removed the K-shell absorption by assuming that
κ decreases as $\omega^{-3.5}$ from an energy just below the K absorption
threshold to 45000 ev and as ω^{-4} afterward (see dashed curve in
Figure 2c), and performed the complete Kramers-Kronig calculation
and sum rules analysis with this modified κ data; we then made a
similar calculation with κ decreasing as $\omega^{-3.5}$ from an energy just
below the L-shell absorption threshold to remove the effects of
both L- and K-shell absorptions (see dashed curve in Figure 2b).
The dashed curves in Figure 14 show the effects on the partial
f-sum rules, giving $n(\infty) \simeq 59.96$ with the K-shell electrons
artificially removed and $n(\infty) \simeq 47.10$ with both and L- and K-
shell electrons artificially removed. We thus obtain 2.60
effective electrons for the K-shell (where there are 4 electrons),
12.86 effective electrons for the L-shell (where there are 16
electrons), and 47.10 effective electrons for the lower energies
(where the 44 M-level, d-band, and valence electrons are contri-
buting; as can be seen from figure 14, the contributions from
these lower levels overlap and cannot be separated as can that
of the deep core levels, in GaAs). Due to Pauli redistribution
of oscillator strength, we do not expect the n_{eff} values for the
various levels to equal the actual number of electrons present;
the expected numbers and the conclusions drawn from matching
these numbers with our calculated results will be discussed in
Section 5.

One more expression, related to the f-sum rules, may be discussed at this point. The logarithmic mean excitation energy I is given by

$$\ln I = \frac{\int_0^\infty \omega \ln\omega \, \text{Im}[\bar{\epsilon}^{-1}(\omega)] \, d\omega}{\int_0^\infty \omega \, \text{Im}[\bar{\epsilon}^{-1}(\omega)] \, d\omega} \quad .$$ (9)

I may be obtained from other optical experiments, for example, stopping power experiments, making this result a particularly useful one for evaluating optical data. We obtain $I \simeq 355.45$ ev.

4. OPTICAL PHONON REGION

In GaAs there is considerable absorption in the far infra-red due to excitation of optical phonons. We have performed some rough calculations that indicate that this absorption contributes only very little to the Kramers-Kronig calculation of the optical constants in the region of electronic excitations, and to the sum rules analysis (the contribution is considerably less than the expected computational uncertainty of the numerical integrations). Thus it is safe to neglect the phonon absorption when the interest is basically in the region of optical electronic excitations. The phonon absorption is interesting in its own right, and we discuss it briefly here in terms of a reflectivity sum rule introduced by Smith and Manogue[18]. Piriou and Cabannes[1] present reflectivity measurements that exhibit a phonon effect

near 0.035 ev; they also present $n(\omega)$ and $\kappa(\omega)$ data in this region, obtained by a partial Kramers-Kronig analysis of their reflectivity data. We used the R-sum rule to evaluate their reflectivity measurements. This R-sum rule can be expressed

$$\frac{1}{\hat{\omega} \ln R_b} \int_0^\infty \ln R(\omega) d\omega = 1, \tag{10}$$

where R_b is the background reflectivity due to the electrons and $\hat{\omega}$ is an energy above that of the phonon effects but below the absorption edge for electronic excitations. We obtain a result of 1.003 for the data of Piriou and Cabannes, using $\hat{\omega} = 0.2$ ev; the R-sum rule is thus obeyed for this data.

5. DISCUSSION

As mentioned earlier, our compilation of the optical
constants of GaAs for incident photon energies in the region
of optical electronic excitations reveals two major discrep-
ancies. We were unable to reproduce the experimental measure-
ments of index of refraction n(hence also reflectivity R and
real part of the dielectric function ε_1) in the region below the
absorption edge, and the analysis by f-sum rules indicates a
lack of oscillator strength in the X-ray region.

We discuss first how the discrepancy in the low energy
region reveals itself. We used experimental measurements[10] of
index of refraction to construct the normal incidence reflec-
tivity curve below the absorption edge (about 1.4 ev in GaAs).
Kramers-Kronig integration then allows us to calculate extinction
coefficient κ for the full range - we do this to obtain values
of κ in the band-to-band region, where absorption cannot be
measured. Subsequently we constructed our "improved" κ curve,
using the above result in the band-to-band region and experimental
values of κ above and below; κ is set equal to zero below the
absorption edge here. Kramers-Kronig integration then results
in a new compilation of all the optical constants - but the
values of R,n, and ε_1 thus created, below the absorption edge,
are about 10% smaller than the experimental values. The more
likely explanations for this are that the measurements of
absorption near the edge, by Sturge[3], give values that are too

small, and/or the normal incidence reflectivity measurements,
in the band-to-band region, by Philipp and Ehrenreich[4], are
too small. We performed some rough calculations to see how large
a change is needed to reproduce the index of refraction measure-
ments, by artificially increasing the values of our "improved"
κ in the questionable regions and examining the results of a
subsequent Kramers-Kronig integration. We note here that the
absorptions in the far infra-red due to optical phonons do not
have a significant effect on the results, and are thus not
expected to be responsible for the discrepancy.

We were able to roughly match the index of refraction
experiments by increasing κ 23% in the region from 2.5 ev to
5.1 ev (we used Philipp and Ehrenreich's[4] R here in the original
calculation); this results in reflectivity values throughout the
band-to-band region that are about 12% larger than the measure-
ments except near the peak at 5 ev, where the difference is about
45%. Increasing κ only in the region of Sturge's measurements
(roughly 1.375 ev to 1.5 ev) was ineffective, requiring a 75%
increase in κ here to increase n below the edge by about 1%
(recall that the discrepancy was about 10%). Increasing κ in
both regions (1.375 ev to 5.1 ev) was more effective; an 18%
increase enabled us to roughly reproduce the n measurements.
The effective increase in R here was about 10% throughout the
band-to-band region (30% near the 5 ev peak). We also evaluated
the sum rules for the latter case; the f-sums gave an n_{eff} value
of 62.76, about 0.2 electrons larger than the original results.

18.

The discrepancy at low energies thus does not account for the lack of oscillator strength (we need to account for about 1.45 electrons).

The lack of oscillator strength, primarily in the X-ray region, may be due to inaccurate and/or inadequate (not enough points to reproduce the structure) measurements in some regions. As discussed earlier, the partial f-sums evaluated using our data indicated that there are 2.60 effective electrons in the K-shell, 12.86 in the L-shell, and 47.10 in the lower levels (M-shell, d-bands, and valence). We calculated the expected oscillator strengths for the various transitions in the Ga and As atoms using Hartree-Fock-Slater atomic wave functions (we utilized the Herman and Skillman Program[19]) and, taking into account Pauli redistribution of oscillator strength, found that the K-shell result should be approximately 2.54 effective electrons, the L-shell result 13.18, and the lower levels 48.28. Due to calculational "noise" and errors inherent in the HFS atomic wave functions, we feel that there is satisfactory agreement in the K-shell, reasonable agreement in the L-shell (could be a small discrepancy, due to inadequate data), and that the lack of oscillator strength must lie primarily in the lower energy X-ray region (extinction coefficient values here must be too small).

The present set of optical constants for GaAs appear to be the best that can be derived from the experimental data presently available. We suggest that experimental values of R, n, and ε_1,

rather than our curves, be used below the absorption edge
(about 1.4 ev); these can easily be obtained for R and n by
drawing a smooth curve through the experimental points in
our Figures 6 and 10, respectively.

Improvements can be made by new measurements of reflectivity
and/or dielectric function in the band-to-band region, and of
absorption in the X-ray region, primarily in the range from
about 150 ev to the onset of L-shell absorptions. (Absorption
measurements elsewhere in the X-ray range would also be help-
ful, as we utilized only Ga and As measurements at energies
above 158 ev). Absorption measurements to better define the
structure just above the L-edge are also required.

REFERENCES

1. Piriou, B., and Cabannes, F., Compt. Rend., Vol. 255, 2932 (1962).

2. Stolen, R.H., Appl. Phys. Letters, Vol. 15. No. 2, 74 (1969).

3. Sturge, M.D., Phys. Rev., Vol. 127, No. 3, 768 (1962).

4. Philipp, H.R., and Ehrenreich, H., Phys. Rev., Vol. 129, No. 4, 1550 (1963).

5. Cardona, M., Gudat, W., Sonntag. B., and Yu, P.Y., Proc. of the 10th Int. Conf. on the Phys. of Semiconductors, Boston, P. 209 (1970).

6. Norelco Reporter (May-June, 1962).

7. Hubble, J.H., McMaster, W.H., Kerr Del Grande, N., and Mallett, J.H., in International Tables for X-Ray Crystallography, P. 47 (Publ. for the Int. Union of Crystallography by the Kynoch Press, Birmingham, England, 1974).

8. Bracewell, B.L., and Veigele, W.J., in Advances in X-Ray Analysis, Vol. 15, ed. by K.F.J. Heinrich, C.S. Barrett, J.B. Newkirk, and C.O. Ruud. P. 352 (Plenum Press, New York, 1972: Conference held Aug., 1971).

9. Henke, B.L., and Ebisu, E.S., in Advances in X-Ray Analysis, Vol. 17, ed. by C.L. Grant. C.S. Barrett. J.B. Newkirk. and C.O. Ruud. P. 152 (Plenum Press, New York, 1973; Conf. held Aug, 1973).

10. Marple, D.T.F., J. Appl. Phys., Vol. 35, No. 4, 1241 (1964).

11. Bearden, J.A., and Burr, A.F., Rev. Mod. Phys., Vol. 39, No. 1, 125 (1967).

12. Panish, M.B., and Casey, H.C., Jr., J. Appl. Phys., Vol. 40. No. 1, 163 (1969).

13. Morrison, R.E., Phys. Rev., Vol. 124, No. 5, 1314 (1961).

14. Clark, G.D., Jr.. and Holonyak. N., Jr., Phys. Rev, Vol. 156, No. 3, 913 (1967)

15. Stern, F., Phys. Rev., Vol. 133, No. 6A, A1653 (1964).

16. Altarelli, M., Dexter, D.L., Nussensveig, H.M., and Smith, D.Y., Phys. Rev. B, Vol. 6, No. 12, 4502 (1972).

21.

17. Smith, D.Y., and Shiles, E., Bull. Am. Phys. Soc., 22, 92 (1977) and Phys. Rev. B, Vol. 17, 4689 (1978).

18. Smith, D.Y., and Manogue, C.A., Bull. Am. Phys. Soc., Vol. 23, No. 3, 342 (1978).

19. Herman, F., and Skillman, S., Atomic Structure Calculations (Prentice-Hall, Inc., Englewood Cliffs, N.J., 1963).

FIGURE CAPTIONS

Fig. 1   Extinction coefficient κ, as function of incident photon energy, for full range of optical electronic excitations.

Fig. 2   (a) Extinction coefficient κ, from 17 ev to 700 ev. The experimental results of Cardona, et al[5], fall on the solid curve up to 158 ev, and the data obtained by an appropriate combination of Ga and As X-ray absorption data, from Henke and Ebisu[9], are shown. (b) Extinction coefficient κ near the onset of L-shell absorption. The combined Ga and As data, taken from the tables of reference 6 and reference 9, are shown. Data taken from references 7 and 8 have been excluded for clarity; these point fall on the solid curve at the higher energy end of this figure. The dashed curve shows an approximate κ with the L- and K-shell electrons artificially removed. (c) Extinction coefficient κ near the onset of K-shell absorption. The combined Ga and As data, taken from the tables of reference 6, are shown; data from references 7 and 8 also fall on this curve. The dashed curve shows an approximate κ with the K-shell electrons artificially removed.

Fig. 3   Extinction coefficient κ in the region of band-to-band excitations. Some of the experimental data, taken from the curves given by Sturge[3] and by Cardona, et al[5], are shown.

Fig. 4   Extinction coefficient κ near the absorption edge. Points taken from the experimental curves given by Sturge[3] and by Panish and Casey[12] are shown.

Fig. 5   Normal incidence reflectivity R for the full range of optical electronic excitations.

Fig. 6   Reflectivity R near the absorption edge. Also shown are data taken from the experimental curves of Philipp and Ehrenreich[4], Marple[10], and Clark and Holonyak[14]. We note that references 10 and 14 give index of refraction n, which converts to R by the expression $R = (n-1)^2/(n+1)^2$ in energy ranges where $\kappa \ll n-1$. The point at $R(\omega=0) = .2858$ is taken from the $n(\omega)$ curve given by Stern[15].

Fig. 7   Reflectivity R in the region of band-to-band excitations. Points taken from the experimental curve of Philipp and Ehrenreich[4] are shown. The dashed curve shows the experimental results of Morrison[13].

Fig. 8   Reflectivity R near the d-band absorption just above 20 ev. Points taken from the experimental curve of Philipp and Ehrenreich[4] are shown. We note that we chose to use the Cardona, et al[5] absorption data in this region rather than the data of reference 4.

Fig. 9   Index of refraction n for the full range of optical electronic excitations.

Fig. 10   Index of refraction n near the absorption edge. Points taken from the experimental curves of Marple[10] and of Clark and Holonyak[14] are shown.

Fig. 11   Real part ε_1 of the dielectric function, for the
           full range of optical electronic excitations.

Fig. 12   Imaginary part ε_2 of the dielectric function, for
           the full range of optical electronic excitations.

Fig. 13   Energy loss function, indicating a peak at the
           plasma frequency of the valence electrons. Our
           results give the plasma frequency at 13.9 ev.

Fig. 14 $n_{eff}(\omega')$ as function of upper limit of integration
           ω', calculated from the three forms of the f-sum
           rule. The dashed curves show the results with the
           K-shell absorption artificiall emoved (upper
           dashed curve) and with both the L- and K-shell
           absorption artificially removed (lower dashed
           curve).

Fig. 1
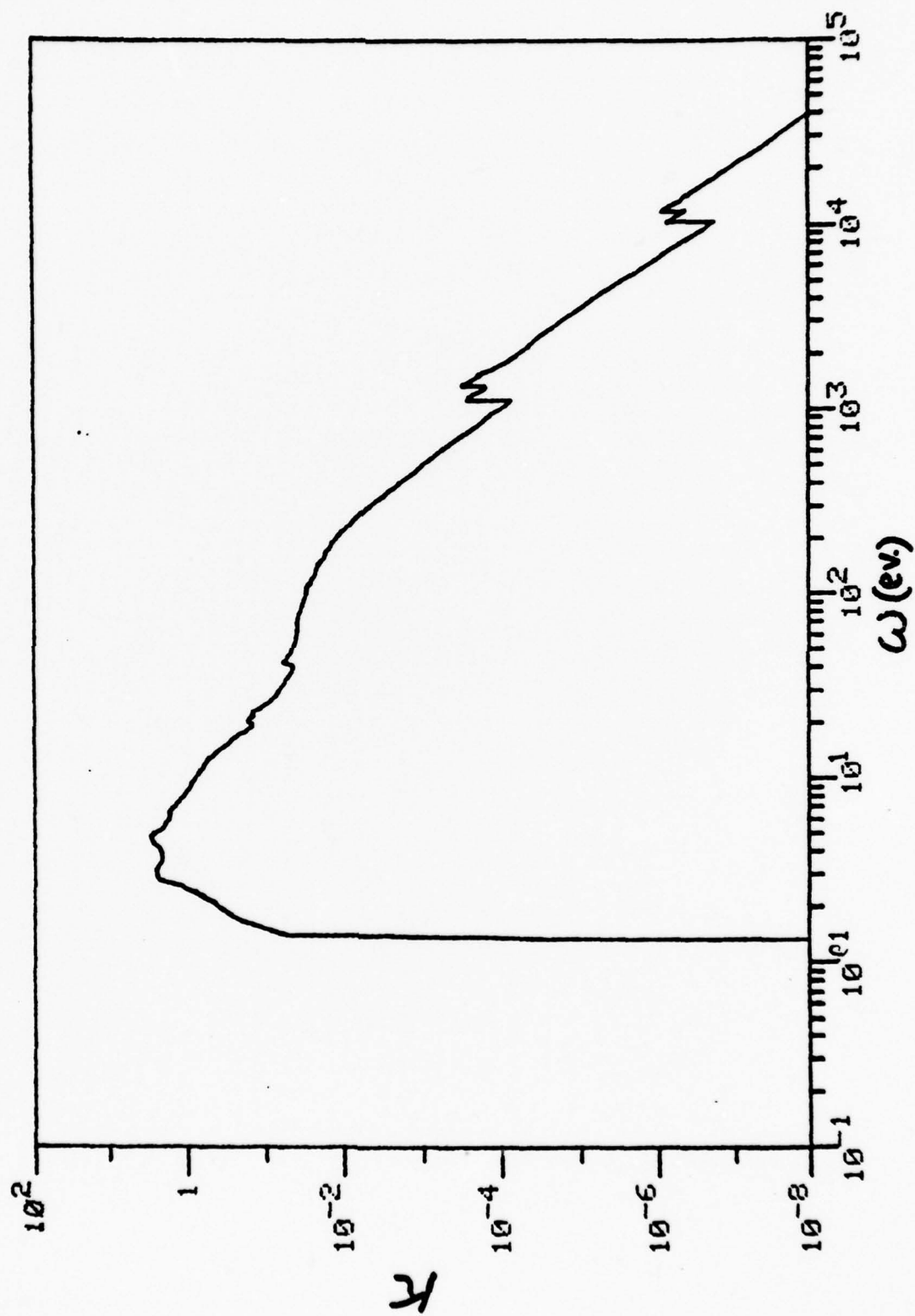
Fig. 2a
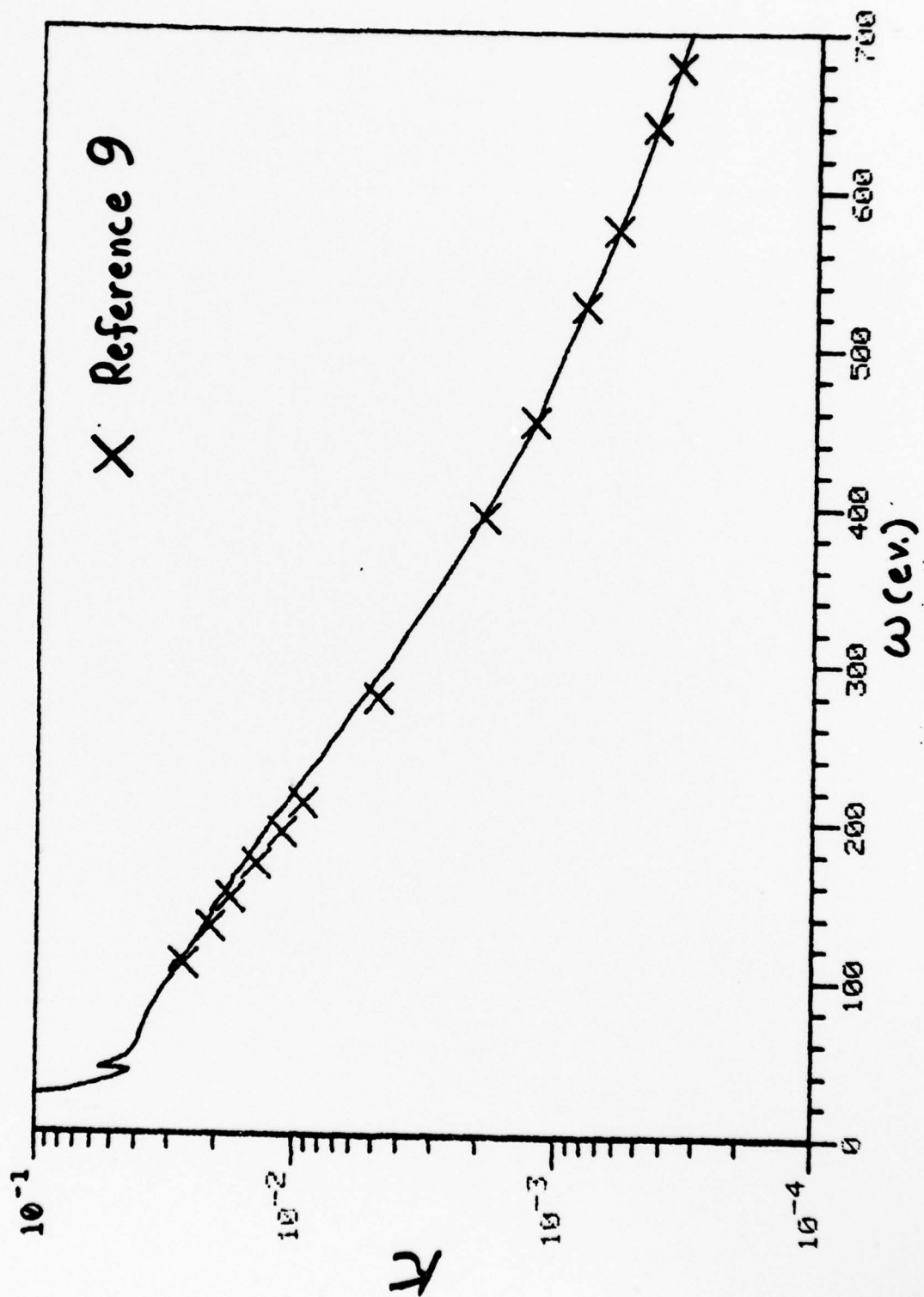
Fig. 2b
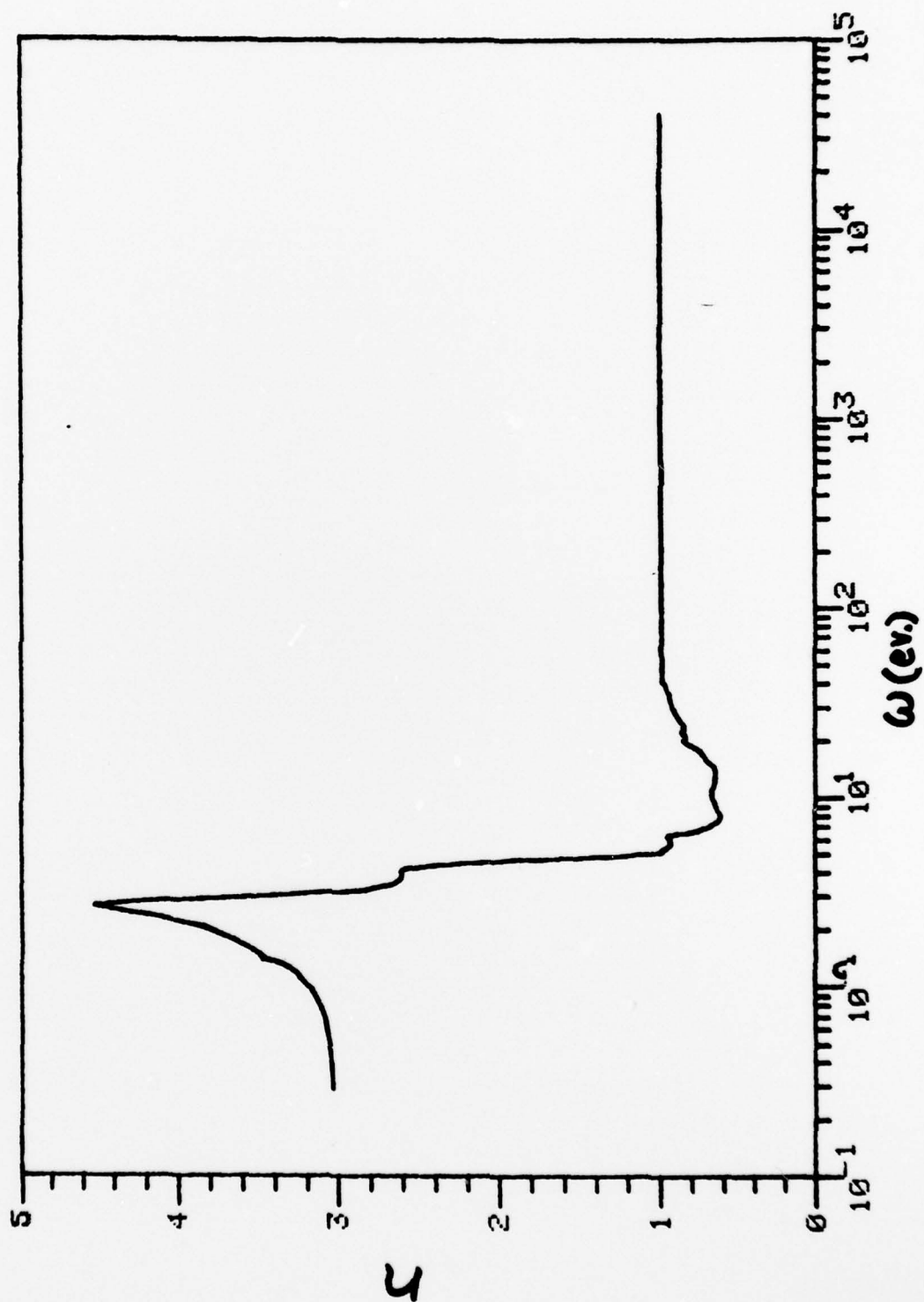
Fig. 2c

△ Reference 6
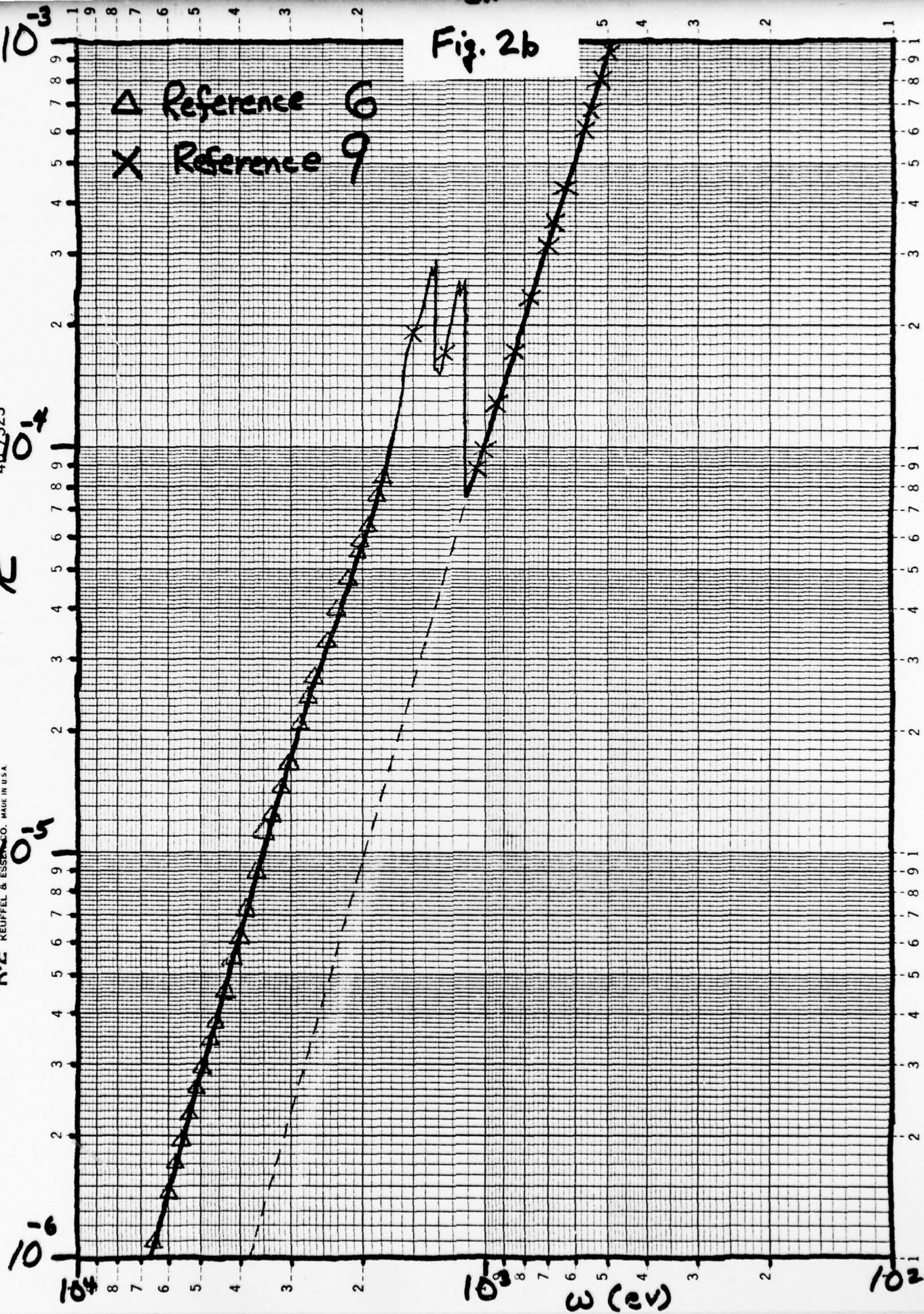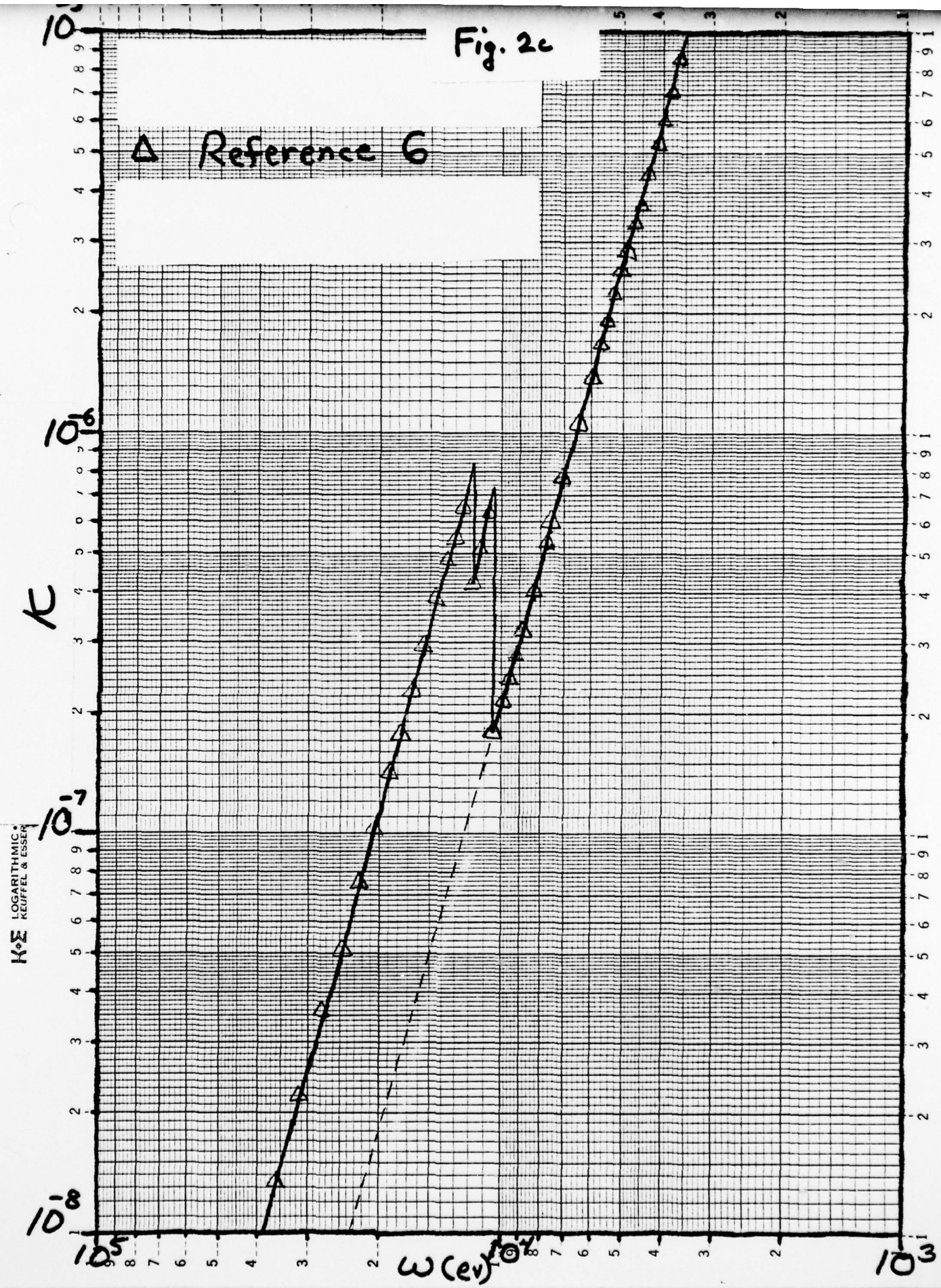
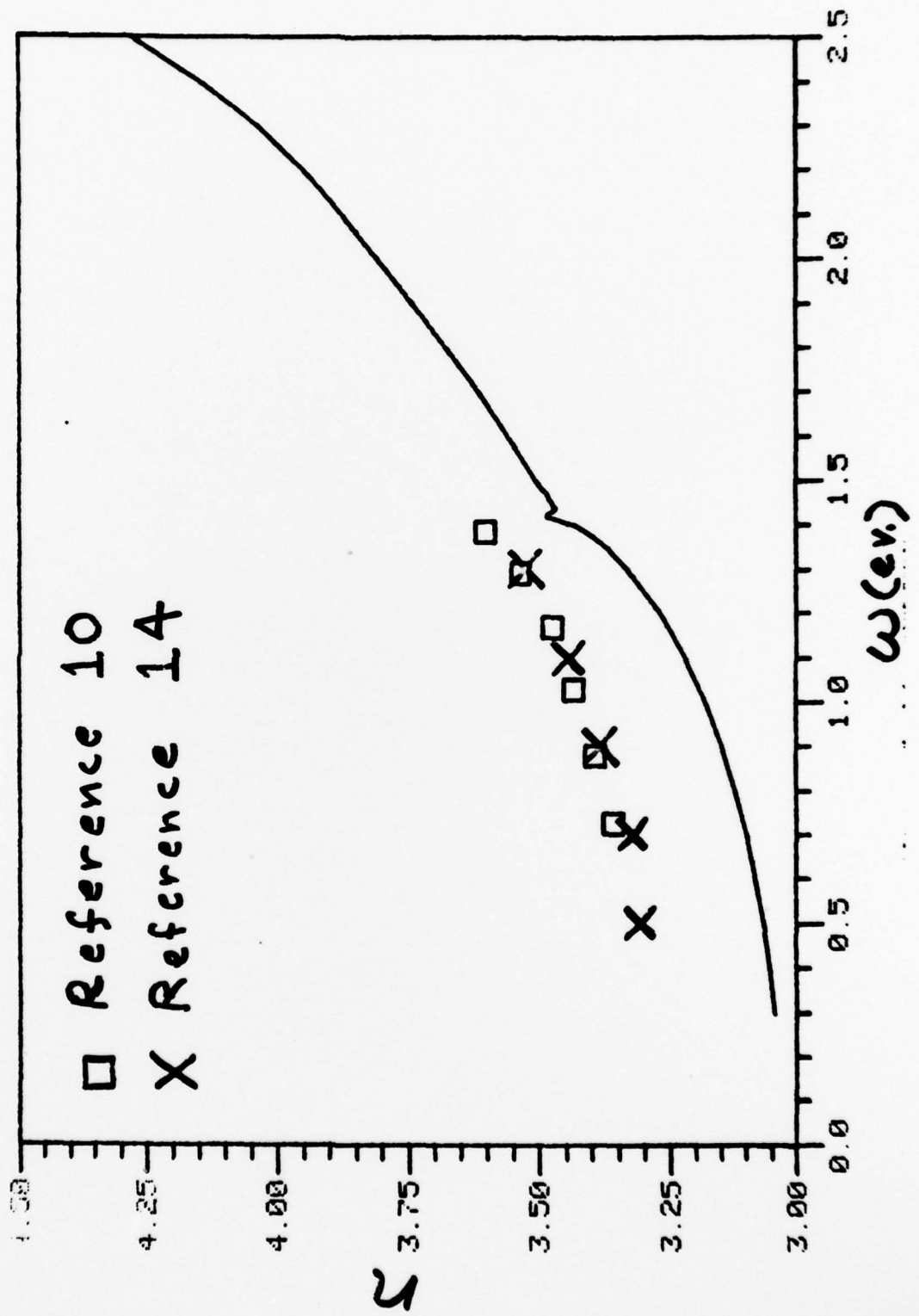# Fig. 3
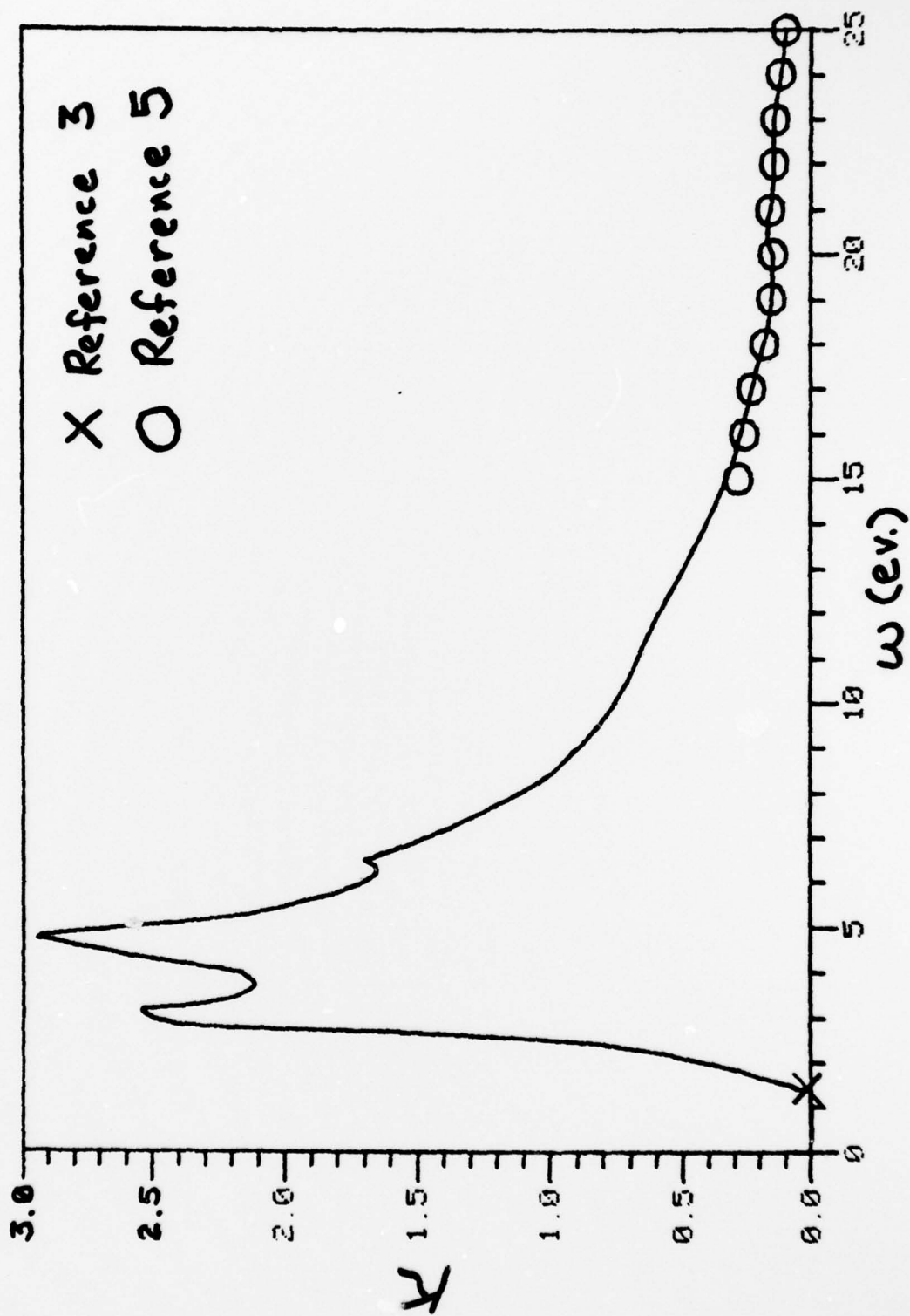
Fig. 4
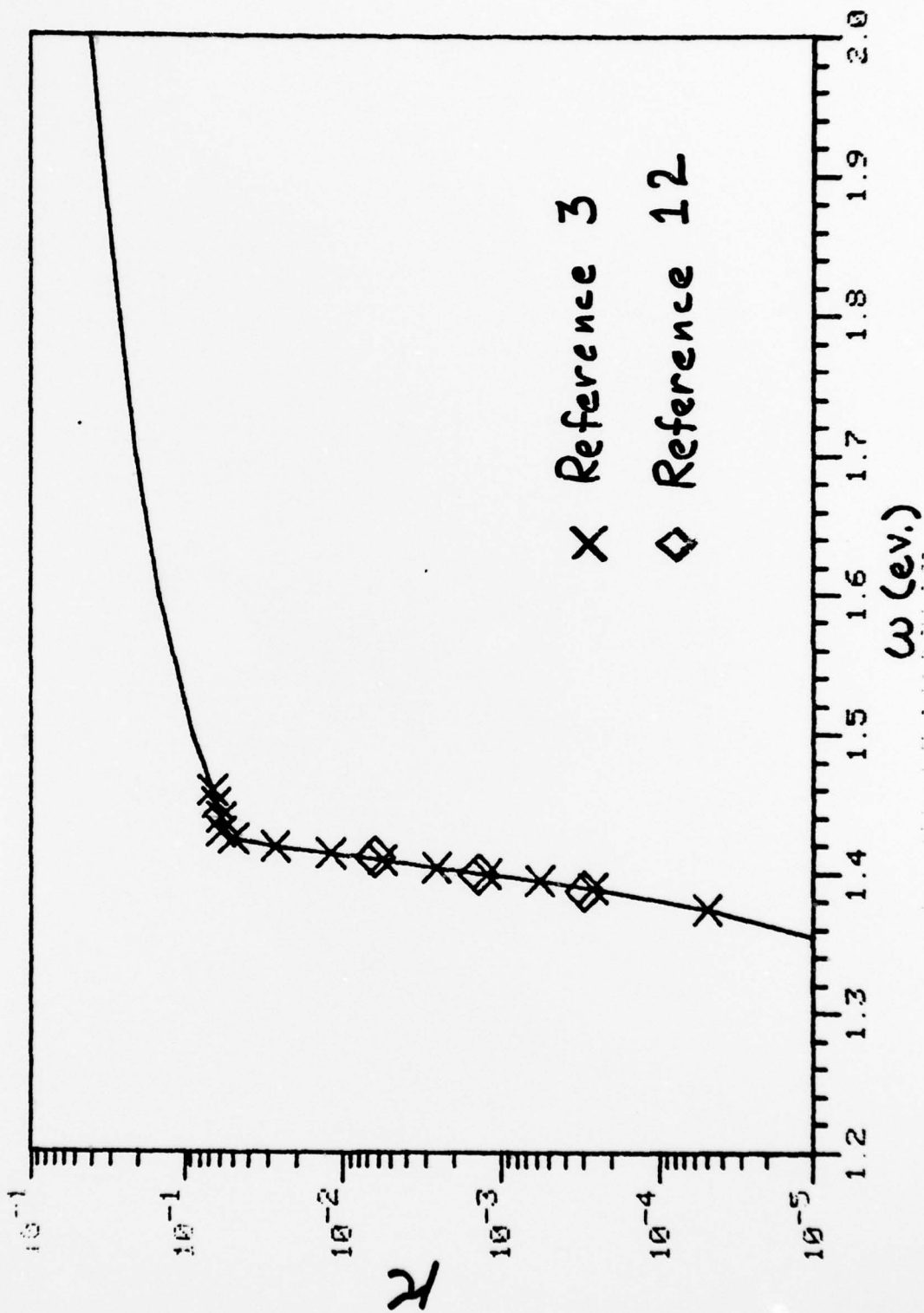
Fig. 5
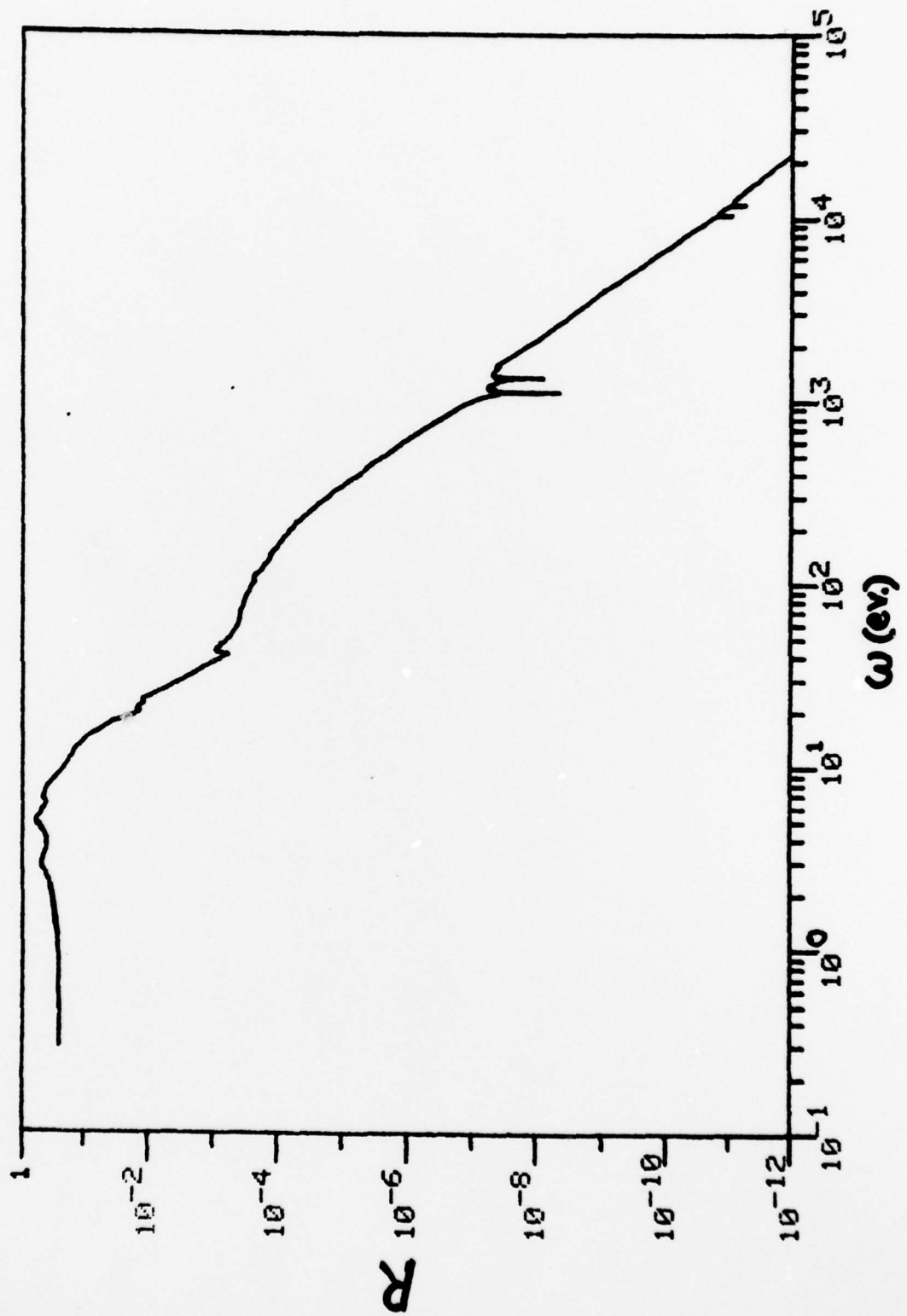
Fig. 6
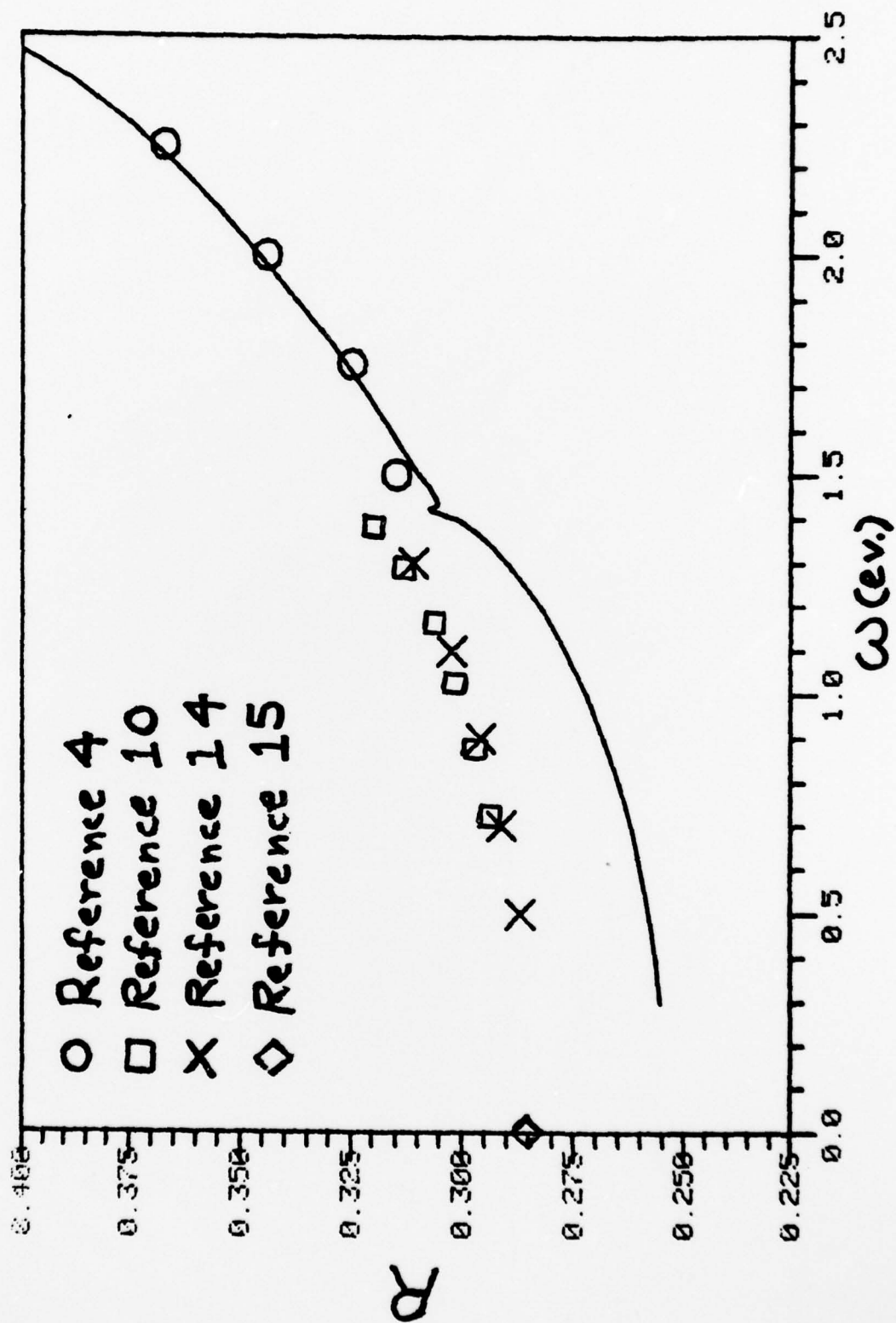
Fig. 7
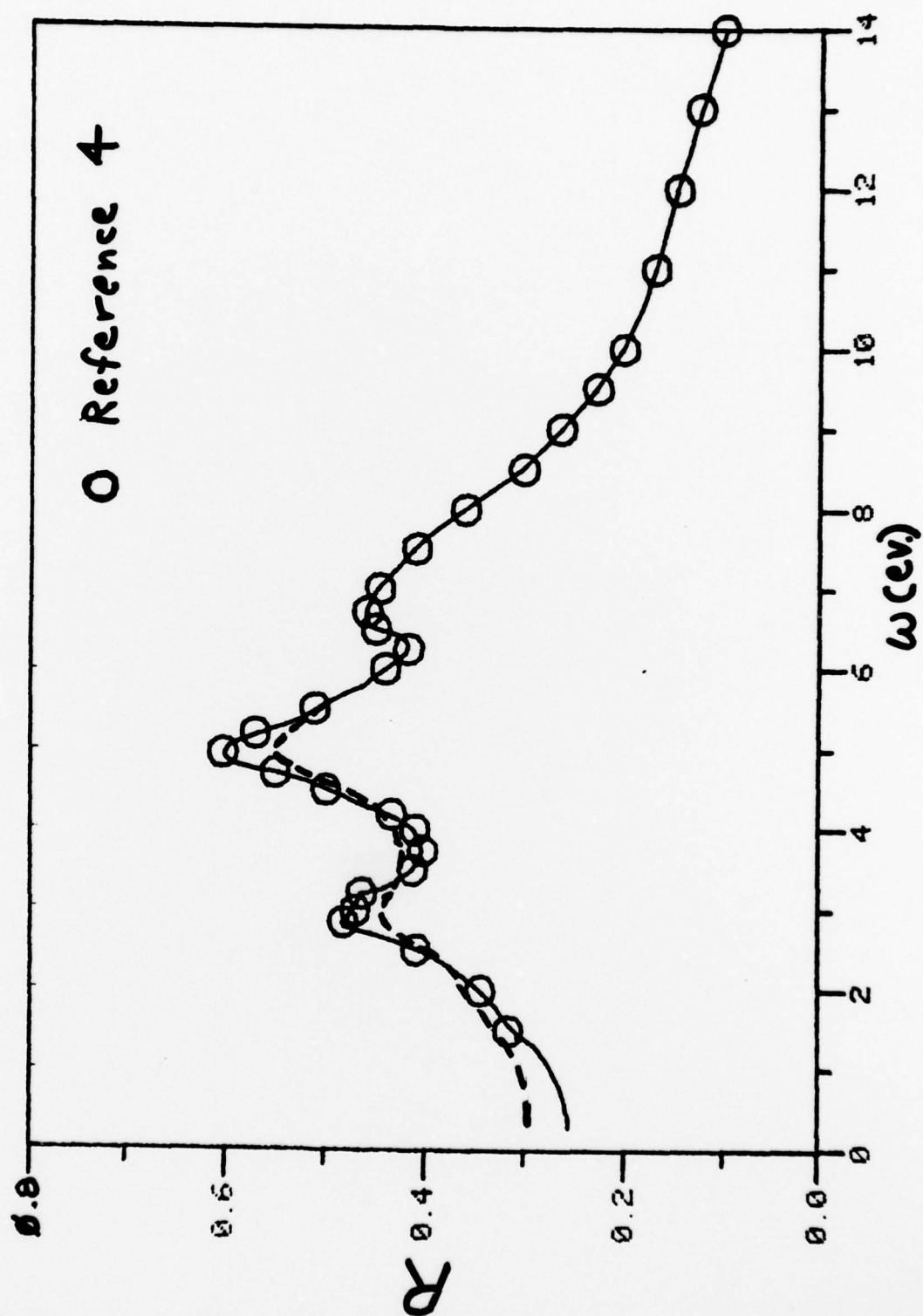
Fig. 8
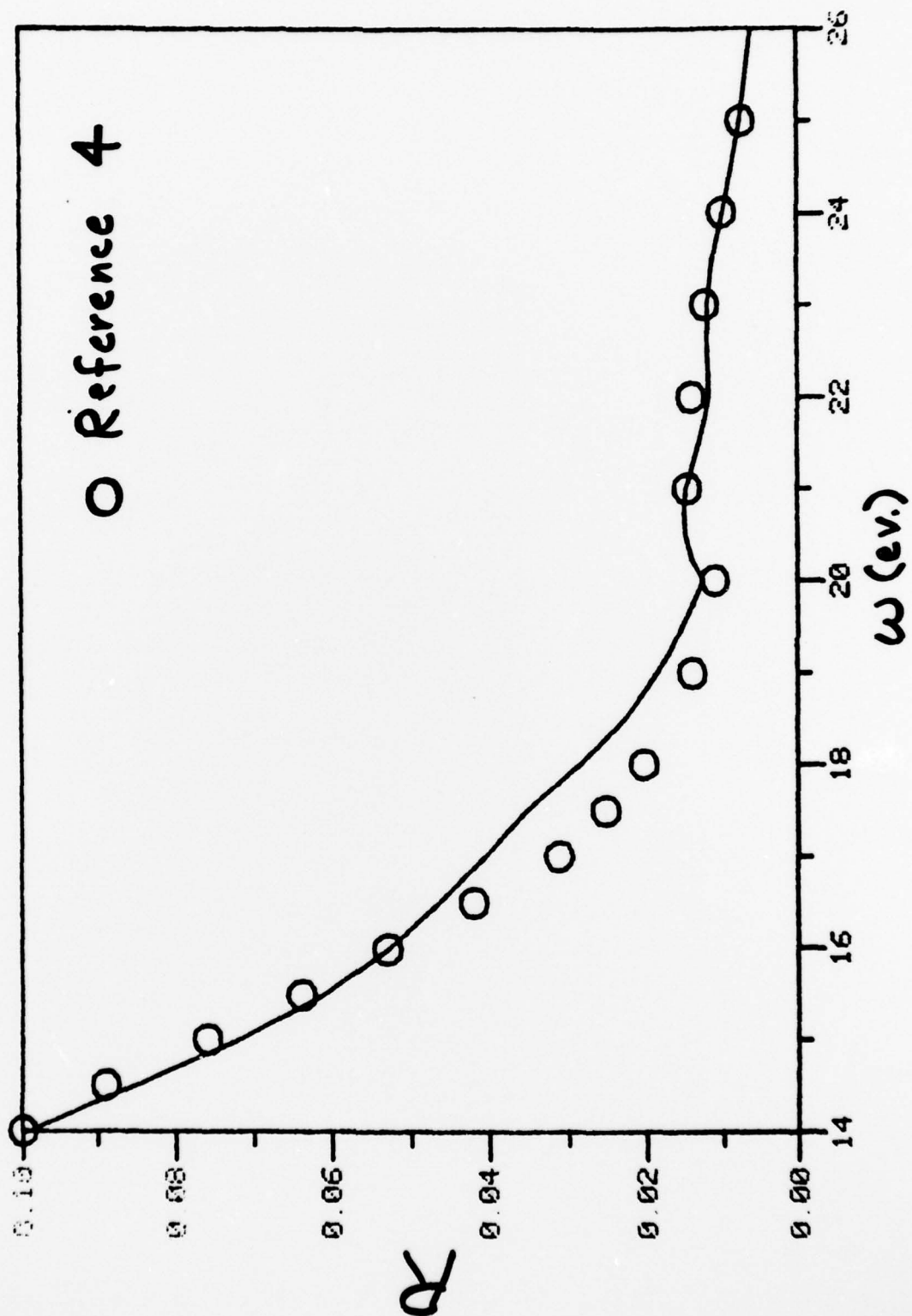
35.

Fig. 9

36.

Fig. 10

Fig. 11

Fig. 12

Fig. 13

Fig. 14